POLITECNICO DI TORINO
Repository ISTITUZIONALE

Integrated LCA and LCC Assessment of a 400 V Automotive IGBT Inverter

Original
Integrated LCA and LCC Assessment of a 400 V Automotive IGBT Inverter / Accardo, A., Calvi, F., Zucca, S.E., Malagrinò, G., Pensato, M., Mosso, S.D., Tinacci, L., Spessa, E.. - In: IEEE ACCESS. - ISSN 2169-3536. - 14:(2026), pp. 162090-162109. [10.1109/ACCESS.2026.3743790]

Availability:
This version is available at: 11583/3017511 since: 2026-11-04T10:08:50Z

Publisher:
Institute of Electrical and Electronics Engineers Inc.

Published
DOI:10.1109/ACCESS.2026.3743790

Terms of use:

This article is made available under terms and conditions as specified in the corresponding bibliographic description in the repository

Publisher copyright

(Article begins on next page)

20 November 2026

IEEE Access
Multidisciplinary | Rapid Review | Open Access Journal

Received 23 September 2026, accepted 9 October 2026, date of publication 14 October 2026, date of current version 26 October 2026.

Digital Object Identifier 10.1109/ACCESS.2026.3743790

RESEARCH ARTICLE

Integrated LCA and LCC Assessment of a 400 V Automotive IGBT Inverter

ANTONELLA ACCARDO[1], FLAVIO CALVI[1], STEFANO E. ZUCCA[2], GIANFRANCO MALAGRINÒ[2], MICHELE PENSATO[2], SILVIO D. MOSSO[2], LEONARDO TINACCI[2], AND EZIO SPESSA[1]

[1]Department of Energy "Galileo Ferraris," Interdepartmental Center for Automotive Research and Sustainable Mobility (CARS), Politecnico di Torino, 10129 Turin, Italy

[2]Dumarey Automotive Italia S.p.A., 10129 Turin, Italy

Corresponding authors: Antonella Accardo (antonella.accardo@polito.it) and Flavio Calvi (flavio.calvi@polito.it)

This work was supported by European Unions Horizon Europe Research and Innovation Program under Grant 101191866.

ABSTRACT This paper focuses on the sustainability analysis of power electronics, particularly on developing an integrated Life Cycle Assessment (LCA) and Life Cycle Costing (LCC) model for an automotive IGBT inverter using SimaPro. The integrated model is parameterized and scalable, enabling the generation of a bill of materials, and environmental and cost-related Life Cycle Inventory (LCI) that adapt according to key parameters such as power and voltage. The model outcomes are environmental impacts and costs of the life cycle of individual inverter components and the inverter itself. A case study has been analyzed, corresponding to a 150 kW and 400 V IGBT inverter mounted on the rear axle of the Volkswagen ID.4. Results highlight that, from an environmental perspective, the aluminum casing, DC-link, and bus bars are the most impactful components. From a cost perspective, the power module is the most significant contributor. Results have been validated through a multi-step validation procedure to assess the robustness of the proposed framework. The LCA results align with the literature in most impact categories, while the cradle-to-gate LCC results deviate by about 16.5% from other benchmark analysis but maintain a consistent trend, demonstrating the models reliability for comparative analysis and margin for future optimization.

INDEX TERMS Inverter, LCA, LCC, sustainability, transportation.

I. INTRODUCTION

One significant barrier to the widespread adoption of electric vehicles (EVs) is their high purchase cost. Many consumers still prefer conventional internal combustion engine vehicles powered by fossil fuels rather than opting for the more environmentally friendly alternative offered by EVs [1]. Potential buyers are unlikely to be influenced by emission savings during vehicle operation, as these are minor compared to the initial purchase price relative to a conventional vehicle [1]. For this reason, economic considerations currently play a crucial role for manufacturers, especially given the moderate growth of the EV market. The cost analysis of power electronics remains important since they play a crucial role in vehicle operation and drive prices.

Furthermore, integrating economic and environmental assessments can yield valuable insights to encourage the adoption of sustainable transportation, as inverters significantly contribute to a vehicle's life cycle emissions, and reveal opportunities for improvement, by enabling the identification of potential criticalities [2]. For instance, [3] explore the application and integration of life cycle assessments (LCAs) in the development of electric drives for automotive purposes. While LCAs are the standard tool for evaluating environmental impacts, Life Cycle Costing (LCC) serves as the economic counterpart, encompassing costs throughout the entire life cycle, including use, end-of-life (EOL), and hidden expenses [4], [5], [6], [7]. Although a product's price typically reflects raw material, production costs, and profit margins, it often excludes costs associated with the use and EOL phases [4]. These later-stage costs can surpass the initial purchase price, particularly in the case of energy-intensive technologies [4]. Lastly, by capturing

The associate editor coordinating the review of this manuscript and approving it for publication was Pinjia Zhang.

© 2026 The Authors. This work is licensed under a Creative Commons Attribution 4.0 License.
For more information, see https://creativecommons.org/licenses/by/4.0/

long-term costs, LCC can support more informed decisions that align with future sustainability goals [4].

For an effective integrated LCA–LCC analysis, consistent system boundaries across all assessments are essential, ideally, they should be identical [8], [9]. This includes aligning on the physical, rather than marketing, life cycle when modeling the Life Cycle Inventory (LCI) [4]. The most robust approach is to use a single, shared LCI as the basis for both environmental and economic assessments [4], [10].

A. STATE-OF-THE-ART AND NOVELTY

Several studies have applied LCA at the system level in the automotive sector. For example, [11], [12] investigate environmental impacts at the drivetrain and vehicle levels, highlighting various sustainability challenges. However, limited attention has been devoted specifically to traction inverter emissions and their contribution to the overall environmental footprint.

Beyond environmental analyses, several studies have focused on techno-economic or performance-oriented assessments of traction inverters and power electronic systems. For instance, [13], [14] evaluate hybrid-switch solutions for traction inverters to balance cost and performance, although without adopting a life cycle perspective. Similarly, integrated analyses combining reliability, cost, efficiency, and power density have been conducted to compare inverter topologies and technologies [15], [16], [17], [18]. Nevertheless, these studies do not explicitly address environmental impacts.

Other contributions have focused on either environmental or economic life cycle analyses alone. A pure LCC analysis of an inverter is presented in [19], focusing on the building sector. On the environmental side, in [20], a pure LCA of a traction inverter is carried out, revealing that manufacturing, dominated by the casing and power module, and the use phase are the two life cycle stages with the highest environmental impact, with mineral resource depletion identified as the most critical contributor. Likewise, [21] employs the LCA methodology to assess the environmental impacts of two electric drives, finding that the IGBT inverter exhibits significant impacts across all indicators, particularly in terms of mineral and metal resource use.

Despite the growing body of literature on environmental and economic assessments, the integration of LCA and LCC remains relatively limited in the field of power electronics. One of the earliest examples is provided by [22], who compare two drive technologies through a combined environmental and economic life cycle analysis. More recently, integrated LCA-LCC approaches have been applied to lightweight EV structural materials [23], battery electric vehicle eco-design and benchmarking studies [24], comparisons of ICEV, HEV, and BEV configurations [25], and assessments of the environmental and economic benefits of BEVs [26]. Integrated LCA-LCC methodologies have also been adopted to evaluate the sustainability of electric traction motors [27] and battery systems [28], [29]. However, applications specifically addressing traction inverters remain scarce, highlighting a significant research gap that motivates the present work.

In this context, the present work develops an integrated LCA-LCC framework for the sustainability assessment of an automotive traction inverter, addressing a gap in the existing literature where traction inverters have primarily been investigated from either an environmental or a techno-economic perspective, but rarely through a jointly constructed life cycle approach.

The framework advances the existing literature through four elements that, to the best of our knowledge, have not been combined before for this class of product. First, a single, fully parameterised Life Cycle Inventory (LCI) feeds both the environmental and the economic assessment, so that consistency in system boundary, functional unit and data structure is guaranteed by construction rather than imposed a posteriori [4], [8], [9], [10]. Second, the only user inputs required are rated power and DC-link voltage, both available at the concept stage from a datasheet, making the model an early-design screening tool rather than a retrospective assessment of an already manufactured unit. Third, results are resolved at the level of individual macro-components and, on the cost side, at the level of individual cost categories (material, process, ancillary, commercial, labour), enabling direct component-by-component comparison of environmental and economic hotspots. Fourth, a three-level validation procedure is applied: component masses against more than 20 commercial inverters, LCIA results against an independent inverter LCA [20] run under identical settings, and life cycle costs against market benchmark data for several EV models.

To demonstrate the applicability of the methodology, a case study is conducted on a 150 kW, 400 V IGBT traction inverter designed to be installed on the rear axle of the Volkswagen ID.4.

II. METHODOLOGY

The LCA was conducted in accordance with ISO 14040 and ISO 14044 standards [30], [31]. While LCA is a well-established and standardized methodology, LCC lacks an equivalent level of standardization. Therefore, in the absence of standardized guidelines for life cycle cost assessment, the methodological structure of LCA was adopted as a reference for the LCC, following recommendations from the relevant literature [32], [33], [34].

Both assessments were developed using identical system boundaries, functional units, and data structures, thereby enabling a consistent evaluation of environmental and economic performance across all life cycle stages. Furthermore, the two analyses followed parallel modelling procedures, from goal and scope definition to inventory compilation and interpretation. This harmonized approach facilitated data integration and result comparison, ensuring methodological consistency and full comparability between environmental impacts and economic costs.

A. GOAL AND SCOPE

The primary objective of this work was to develop a parameterized LCA-LCC model for the integrated assessment of the environmental impacts and costs of automotive IGBT inverters throughout their life cycle within the SimaPro environment. The model was designed to maximize usability by relying on a limited set of readily available input parameters, namely rated power and voltage, which can be easily retrieved from the literature or manufacturers' datasheets.

This parameterization makes the framework highly flexible and adaptable to different application contexts. By simply specifying the inverter power and voltage ratings, users can automatically generate the corresponding BoM and evaluate both the environmental impacts and life cycle costs of the system. To further improve usability, the model was developed with a straightforward and intuitive structure, enabling users to input parameters correctly and efficiently while minimizing modelling complexity.

The parameterized model covers the cradle-to-gate system boundary (Figure 1), encompassing all stages from raw material extraction and processing to the manufacturing of the finished product. The use and end-of-life phases of the inverter were incorporated only in the case study through dedicated LCI modelling to cover the cradle-to-grave boundary (Figure 1). This approach was adopted due to the limited availability of data suitable for parameterization across the entire cradle-to-grave boundary.

To carry out the analysis, SimaPro software version 9.3.0.3 was used, with Ecoinvent 3.8 as the background database.

The definition of the functional unit is a critical step in life cycle assessment, as it should accurately reflect the function of the product under study [30].The primary function of a traction inverter is to convert direct current (DC) from the battery into variable-voltage, variable-frequency three-phase alternating current (AC) to drive the electric motor. Conversely, during regenerative braking, it converts three-phase AC generated by the motor back into DC for battery charging [36], [37]. At the same time, traction inverters are intermediate products supplied to Original Equipment Manufacturers (OEMs), making it challenging for component manufacturers to directly relate their product to the final vehicle-level function. For this reason, the functional unit adopted in this study is defined as one traction inverter, whose characteristics and mass are determined by the input design parameters, namely rated power (kW) and DC-link voltage (V). This definition reflects the perspective of the component supplier while ensuring consistency with the parameterized modelling approach.

B. CASE STUDY

The case study is the IGBT inverter mounted on the Volkswagen ID.4 rear-wheel drive (RWD), whose main specifications are reported in Table 1. Based on the available primary data, it was possible to retrieve the nominal power (150 kW) and voltage (400 V) of the selected case study. Also, the inverter under study has liquid cooling system. Specifically, the aluminium housing, cold plate with cooling channels, sealing and coolant fittings, and thermal interface material are included and modelled as part of the casing macro-component, while the vehicle-level thermal management circuit (coolant pump, radiator, hoses, expansion tank, and coolant charge) is excluded, with the justification that these components are shared with the e-motor and battery thermal circuit and cannot be allocated to the inverter consistently with the adopted functional unit. The case study has an overall

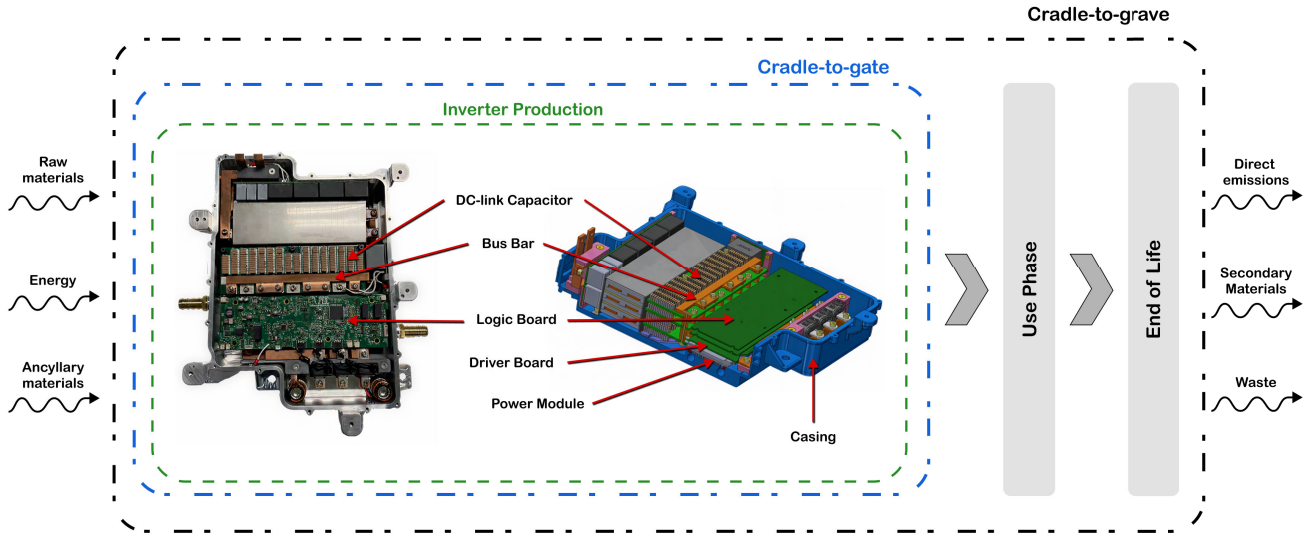


FIGURE 1. System boundary. Picture adapted from [35].

mass of about 8–10 kg with the inclusion of both casing and bus bars.

TABLE 1. Main technical characteristics of the reference inverter case study.

Parameter	Value	Reference
Reference vehicle	VW ID.4 RWD	
Inverter type	IGBT	[38], [39]
Specified nominal power	150 kW	[38]
Specified battery voltage	400 V	[39]
Housing	Included	Assumed
Bus bar	Included	Assumed
Type of coolant	Liquid	[40]

C. LIFE CYCLE INVENTORY

The parametrization was carried out according to the principles and scaling relations defined in [41], which provide a structured methodology to estimate, from rated power and DC-link voltage alone, the masses of the individual components constituting the inverter, including the power module, DC-link capacitor, bus bars, casing, logic board, and driver board, as well as the quantities of consumables and ancillary materials used during manufacturing, such as solvents, coolants, and solder, which do not form part of the final product but contribute to its environmental and cost inventory. The resulting model is valid within an applicability range of 20 to 200 kW rated power and 250 to 700 V DC-link voltage, covering the large majority of current automotive IGBT traction inverter designs. High-voltage IGBTs for railway, industrial and grid applications are outside the scope of the study.

1) LCA MODEL

For the LCA, all the material and energy flows in and out of each unit process were evaluated during the inventory phase. To address the problem under investigation, a literature review was conducted to identify relevant data. For example, [41] provides an overview of the assembly processes and treatments, such as cleaning, plating, rinsing, soldering, as well as electricity consumption, emissions, and waste streams that contribute to the production of an inverter unit. In the absence of more detailed data, the model was constructed assuming global geographic averages. The end-of-life stage was modelled through two distinct processes. First, the aluminium casing is treated through a recycling process modelled from scratch, assuming a recycling efficiency of 83.7%, consistent with current industrial practice for post-consumer aluminium recovery. Second, the electronic waste, is assumed to be treated accounting for transport to the treatment facility, facility infrastructure, energy consumed during shredding, and the resulting direct emissions to soil and air. In terms of granularity, the model is nested and structured by dividing the inverter into macrocomponents (e.g., logic board, driver board, DC-link capacitor, power modules), which were further organized into additional categories and subcategories.

2) LCC MODEL

The LCC analysis was likewise implemented in SimaPro. While the software was not specifically developed for cost assessments, it provides sufficient functionality to support life cycle costing studies and the evaluation of economic aspects alongside environmental impacts [42]. Accordingly, the cost model was structured around three main components: the base cost (C_{base}), the commercial cost (C_{com}), and the labour cost (C_{lab}). The base cost was calculated as the sum of material, manufacturing process, and ancillary material costs, according to Equation 1.

$$C_{\text{base}} = C_{\text{mat}} + C_{\text{proc}} + C_{\text{anc}} \tag{1}$$

where C_{mat} is the raw material cost [EUR/piece], C_{proc} is the manufacturing process cost [EUR/piece] and C_{anc} is the cost of ancillary materials [EUR/piece]. More details on these cost categories are reported in. Whenever suppliers provided quantity-dependent pricing, volume discounts were incorporated to improve the representativeness of the cost estimates. The production scenario assumed an average manufacturing volume of 10,000 inverter units per month, corresponding to approximately 100,000 units per year.

Commercial costs were represented through a fixed overhead factor α, accounting for indirect expenses such as administration, logistics, sales, and profit margins. In the absence of detailed company-specific financial data, α was conservatively set to 20%, consistent with common engineering cost-estimation practices.

$$C_{\text{com}} = \alpha C_{\text{base}} \tag{2}$$

The labour cost, C_{lab}, was calculated based on [43]. The model combines direct labour cost, fixed cost, and variable cost as reported in Equation 3, and was implemented consistently with the adopted LCA framework. The labour cost model includes the cost contributions associated with PCB-related mounting process and inverter assembly operations. Therefore, the unit labour cost is expressed as the sum of these two cost components, each obtained from the contribution of the different manufacturing operations, as reported in Equation 4 and 5.

$$C_{\text{lab}} = \frac{C_{\text{PCB}} + C_{\text{INV}}}{Q_{\text{pce}}} \tag{3}$$

$$C_{\text{PCB}} = \sum_{i=1}^{n_{\text{PCB}}} \left(C_{i,\text{dir}}^{\text{PCB}} + C_{i,\text{fix}}^{\text{PCB}} + C_{i,\text{var}}^{\text{PCB}} \right) \tag{4}$$

$$C_{\text{INV}} = \sum_{j=1}^{n_{\text{INV}}} \left(C_{j,\text{dir}}^{\text{INV}} + C_{j,\text{fix}}^{\text{INV}} + C_{j,\text{var}}^{\text{INV}} \right) \tag{5}$$

where C_{lab} is the unit labour cost [EUR/piece], C_{PCB} and C_{INV} are the annual cost contributions related to PCB operations and inverter assembly operations, respectively, and Q_{pce} is the annual production volume. The summations account for the different operations included in each cost block, while the terms C_{dir}, C_{fix}, and C_{var} represent the corresponding direct labour, fixed, and variable cost contributions.

The assessment considers average global wage levels for production activities, a three-shift working schedule, and an annual production volume of $Q_{\text{pce}} = 100{,}000$ inverter units/year. Based on this cost model, the resulting labour cost was estimated equal to $C_{\text{lab}} = 18$ EUR/piece.

Finally, the total inverter cost was obtained by summing the base, commercial, and labour cost contributions:

$$C_{tot} = C_{\text{base}} + C_{\text{com}} + C_{\text{lab}} \tag{6}$$

Commercial and labour costs were modelled separately from material- and process-related costs because they are not directly linked to the mass of the inverter components and therefore cannot be reliably estimated through mass-based scaling relationships.

All cost unit contributions that make up the inverter were considered, always referenced to a physical quantitative unit such as mass, volume, or surface area. A cost database was constructed using literature data, online supplier catalogs, and internal benchmarking studies such as [44], [45], [46], and [47]. These cost units were then assigned to the respective quantities, resulting in an LCC model capable of scaling according to user inputs such as power and voltage. This parametrization allows the economic aspect to adjust alongside the physical characteristics of the inverter.

Currency conversion (e.g., EUR/USD) was applied to prices where necessary, and the exchange rate period was June-September 2025. Cost results are representative of the market conditions of 2025 and their validity can reasonably be assumed for a window of approximately two to three years, i.e. up to 2027–2028, provided that no structural discontinuity occurs in the commodity or semiconductor markets.

D. LIFE CYCLE IMPACT ASSESSMENT

The LCIA was performed by applying the Environmental Footprint (EF) 3.0 method, whose impact categories are reported in Table 2. This method represents a widely recognized and commonly used standard, established by the European Union in 2013 with the aim of assessing and communicating LCA study results in a consistent manner [48]. The subsequent interpretation phase included checks and corrections aimed at addressing model limitations, promoting iterative improvement, and deriving robust conclusions and recommendations [49].

III. RESULTS

This section presents the results of the proposed LCA-LCC model. First, the results obtained for the case study are discussed. Subsequently, the model outputs are validated through comparisons with both literature data and benchmark data.

A. CASE STUDY RESULTS

The results of the LCA of the case study are illustrated in Figure 2. Each bar shows an impact category and its impact breakdown in percentage based on the different components that constitute the inverter under study (e.g., power module, DC-link capacitor, casing). The results highlight that the casing, DC-link capacitor, and bus bars are the main contributors to the majority of environmental impact categories.

TABLE 2. Impact categories within the EF3.0 method and corresponding units of measure.

Impact Category	Unit of measure
Climate change (GWP)	kg CO_2 eq
Ozone depletion (OD)	kg CFC11 eq
Ionising radiation (IR)	kBq U-235 eq
Photochemical ozone formation (POF)	kg NMVOC eq
Particulate matter (PM)	disease inc.
Human toxicity, non-cancer (HTNC)	CTUh
Human toxicity, cancer (HT)	CTUh
Acidification (TAP)	mol H^+ eq
Eutrophication, freshwater (FE)	kg P eq
Eutrophication, marine (ME)	kg N eq
Eutrophication, terrestrial (TE)	mol N eq
Ecotoxicity, freshwater (FET)	CTUe
Land use (LU)	Pt
Water use (WD)	m^3 depriv.
Resource use, fossils (FD)	MJ
Resource use, minerals and metals (MRD)	kg Sb eq

Regarding GWP, the main carbon footprint hotspots are the casing (with a 44% contribution) and the DC-link capacitor (30%). The climate change hotspot of the casing is due to the fact that primary aluminium production is extremely electricity-intensive, and the electricity mix is highly significant [50]. In this study, primary aluminium is assumed to be sourced from the so-called Rest-of-the-World (RoW) region, which represents the emissions of primary aluminium production in all countries not included in the EU27 & EFTA region of the International Aluminium Institute (IAI) classification. Currently, aluminium is mainly produced using electricity from fossil-fueled power plants, so decarbonizing electricity production through low-emission power sources is crucial for primary aluminium production [51]. Of course, aluminium recycling would completely change the scenario [52], as would aluminium lightweighting due to its integration in the drivetrain, by reducing the surface area and volume needed for a separate aluminium casing. In DC-link capacitors, the climate hotspot is largely the manufacturing and materials burden of the capacitor itself. The introduction of secondary aluminium and copper into the final product would be significantly beneficial [53].

Regarding other environmental impact categories beyond GWP, bus bars emerge as significant contributors to issues like human toxicity, acidification, freshwater eutrophication, freshwater ecotoxicity, mineral and metal resource consumption, and land use. These components are rich in metals, meaning their environmental impact is more influenced by the production of metals upstream, particularly the extraction, refining, and semi-fabrication of copper or aluminium, rather than their operational use. The production of copper is linked to pathways of heavy-metal contamination in both terrestrial and marine ecosystems. Additionally, the adverse health effects on humans from copper mining and production are

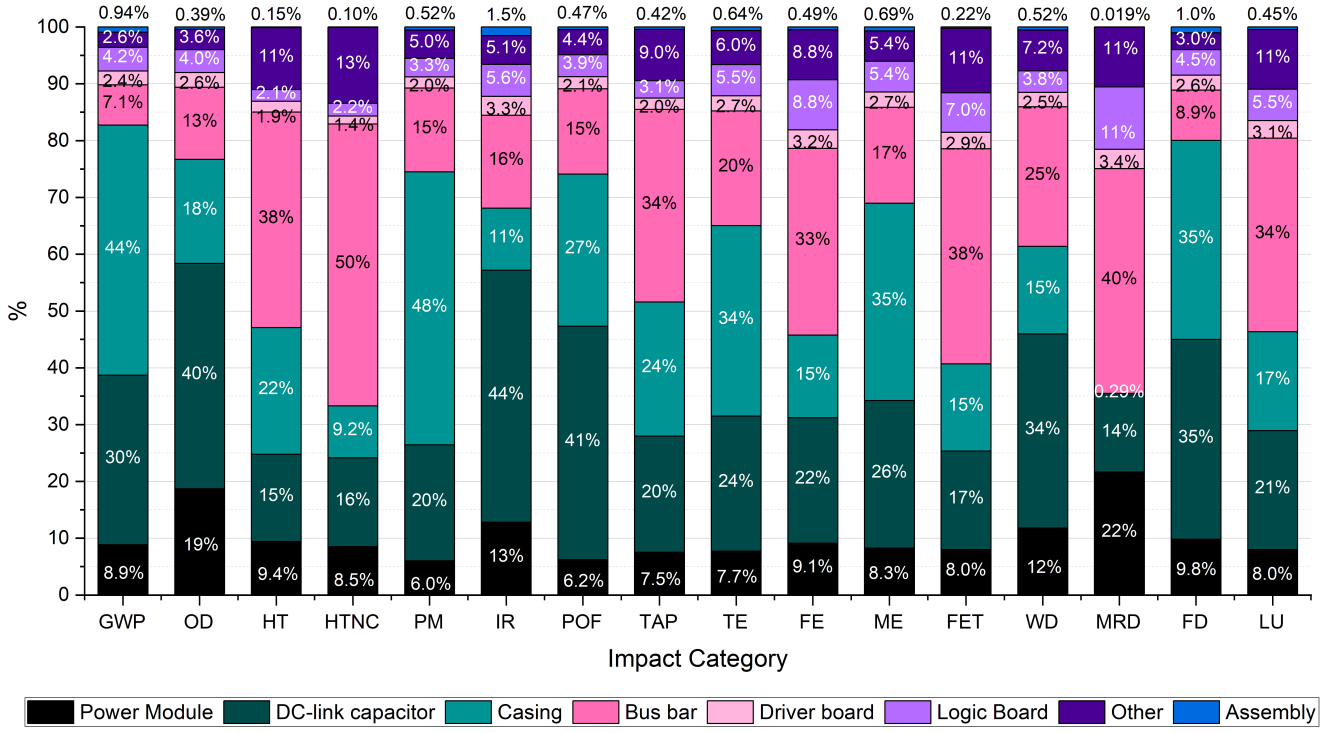


FIGURE 2. LCA results of the case study from the constructed model (percentage contributions of each component).

due to the toxicity of heavy metals such as antimony, arsenic, cadmium, chromium, zinc, nickel, and mercury [54].

While the power modules have a minor (8.9%) contribution to GWP, their contribution increases and becomes significant (>10%) in ozone depletion, ionising radiation, and resource use of minerals and metals. Ozone depletion and ionizing radiation is mainly due to silicon wafer fabrication (76% and 63%), while resource use of minerals and metals is mainly due to antimony used in lid and frame (67%). In fact, power modules rely on critical raw materials, specialised substrates, and rare earth elements that require mining and refining.

Table 3 reports the absolute values for each impact category. The case study inverter has a carbon footprint of 445 kgCO2eq in the cradle to gate boundary, and 1366 kgCO2eq in the cradle to grave boundary.

Figure 3 presents the environmental impact of the case study in the cradle to grave boundary by detailing the percentage contribution of each life-cycle phase across

TABLE 3. LCA results for the case study from the constructed model (absolute total values).

Impact category	Unit	Cradle to gate	Cradle to grave
Climate change	kg CO_2 eq	4.45E+02	1.37E+03
Ozone depletion	kg CFC11 eq	3.77E-05	9.70E-05
Ionising radiation	kBq U-235 eq	4.00E+01	5.69E+02
Photochemical ozone formation	kg NMVOC eq	2.29E+00	4.49E+00
Particulate matter	disease inc.	3.11E-05	4.95E-05
Human toxicity, non-cancer	CTUh	4.39E-05	5.62E-05
Human toxicity, cancer	CTUh	8.20E-07	1.22E-06
Acidification	mol H^+ eq	5.06E+00	1.04E+01
Eutrophication, freshwater	kg P eq	4.06E-01	1.35E+00
Eutrophication, marine	kg N eq	5.81E-01	1.50E+00
Eutrophication, terrestrial	mol N eq	6.27E+00	1.43E+01
Ecotoxicity, freshwater	CTUe	3.65E+04	5.14E+04
Land use	Pt	2.07E+03	6.17E+03
Water use	m^3 depriv.	1.41E+02	4.41E+02
Resource use, fossils	MJ	5.34E+03	2.50E+04
Resource use, minerals and metals	kg Sb eq	1.00E-01	1.09E-01

selected impact categories. The phases considered are materials and manufacturing (black), transport and distribution (dark teal), use phase (teal), and end-of-life treatment (pink).

The use phase emerges as the primary contributor across most impact categories. For GWP, it accounts for 63% of the total impact, reflecting the significant influence of operational energy consumption and energy losses on the inverters climate-change performance. This phases contribution is even more pronounced for ionising radiation and fossil resource use, exceeding 70% of the total impact. The environmental hotspot associated with the use phase is driven by the electricity mix selected for modelling the operational stage. Since the inverter does not produce direct emissions during operation, its environmental burden is primarily associated with the electricity required to compensate for conversion losses over its lifetime. Therefore, the impacts of this phase are strongly influenced by the carbon and resource intensity of the electricity supply. In this study, the average European electricity mix was considered, which includes renewable, fossil-based, and nuclear electricity generation [55]. According to the results, fossil-based generation contributes directly to GHG emissions, while the nuclear share of the mix can influence the ionising radiation indicator and fossil resource depletion through upstream nuclear-related processes. As a result, the use-phase impacts are transferred upstream to the electricity generation system rather than occurring directly at the inverter level. This explains why operational energy losses are responsible for a substantial share of the overall environmental footprint, particularly for GWP, ionising radiation, and resource use, fossils. The results also indicate that reducing inverter losses and adopting a lower-carbon electricity mix would be key strategies to decrease the life-cycle impacts of the system [56].

Materials and manufacturing also contribute substantially to GWP, representing about 30% of the total impact. This is mainly attributed to key components such as the casing and DC-link capacitor, consistent with the findings in Figure 2. For other impact categories, including resource use (minerals and metals), human toxicity (non-cancer), and freshwater ecotoxicity, this phase dominates, contributing over 70% of the impact. Transport and distribution have a negligible effect across all categories, generally below or close to 1%. The end-of-life phase offers environmental credits in several categories, such as GWP, particulate matter, photochemical ozone formation, acidification, and terrestrial eutrophication, primarily due to material recovery and recycling. However, it also results in positive environmental burdens in categories like ozone depletion, water use, land use, and mineral and metal resource use.

Figure 4A shows the total cost breakdown of the case study both in absolute terms and as percentages, by highlighting the percentage contribution of base cost, labour cost, and commercial cost. The overall cost amounts to € 520.3, where the base cost is the dominant contribution, accounting for 81% of the total. The commercial cost is the second-largest contribution, equal to 16% of the total cost, while the labour cost has only a marginal impact.

Figure 4B shows the base-cost breakdown in both absolute values and percentages. The inverter cost is highly concentrated in a small number of components. The power module is the dominant cost driver, accounting for 37% of the base cost, followed by the logic board (16.4%). Together, these two components represent nearly the half of the overall base cost of 418€, indicating that cost-reduction strategies should primarily target the power module.

The high cost of IGBT power modules is largely attributable to their complex multi-chip packaging. These modules integrate semiconductor dies, insulating substrates, interconnections, and cooling structures while meeting stringent reliability and thermal-management requirements [57], [58]. Their price is further influenced by the use of specialized semiconductor materials and the advanced engineering needed to ensure safe and reliable operation. In particular, silicon wafer prices have a direct impact on IGBT manufacturing costs [59].

From a supply-chain perspective, the semiconductor industry is characterized by a high degree of concentration, making it vulnerable to disruptions that can increase production costs and create shortages [60], [61]. A notable example was the COVID-19 pandemic, during which semiconductor plant shutdowns contributed to a global automotive chip shortage [61], [62]. Moreover, IGBT production requires highly precise fabrication processes, including advanced doping techniques and strict cleanroom conditions, both of which significantly increase manufacturing expenses.

As reported by [63], equipment and capital expenditures constitute the largest share of costs in integrated-circuit manufacturing, increasing complexity in new power plant build up.

Growing demand from sectors such as electric vehicles and renewable energy installations has also contributed to rising IGBT module prices [64], [65]. Consequently, considerable research efforts have focused on improving module packaging to achieve more effective thermal management, robust interconnections, enhanced mechanical support, greater reliability, compactness, and lower production costs [66].

Reducing the cost of power modules remains a critical challenge for improving the affordability of electric vehicles. According to [66], innovative device architectures, such as reverse-conducting (RC) and reverse-blocking (RB) IGBTs, can reduce module volume and weight, thereby lowering overall costs. Similarly, integrated liquid-cooled IGBT modules are particularly attractive for automotive applications due to their superior thermal performance and favorable trade-offs in terms of size, weight, and cost [66].

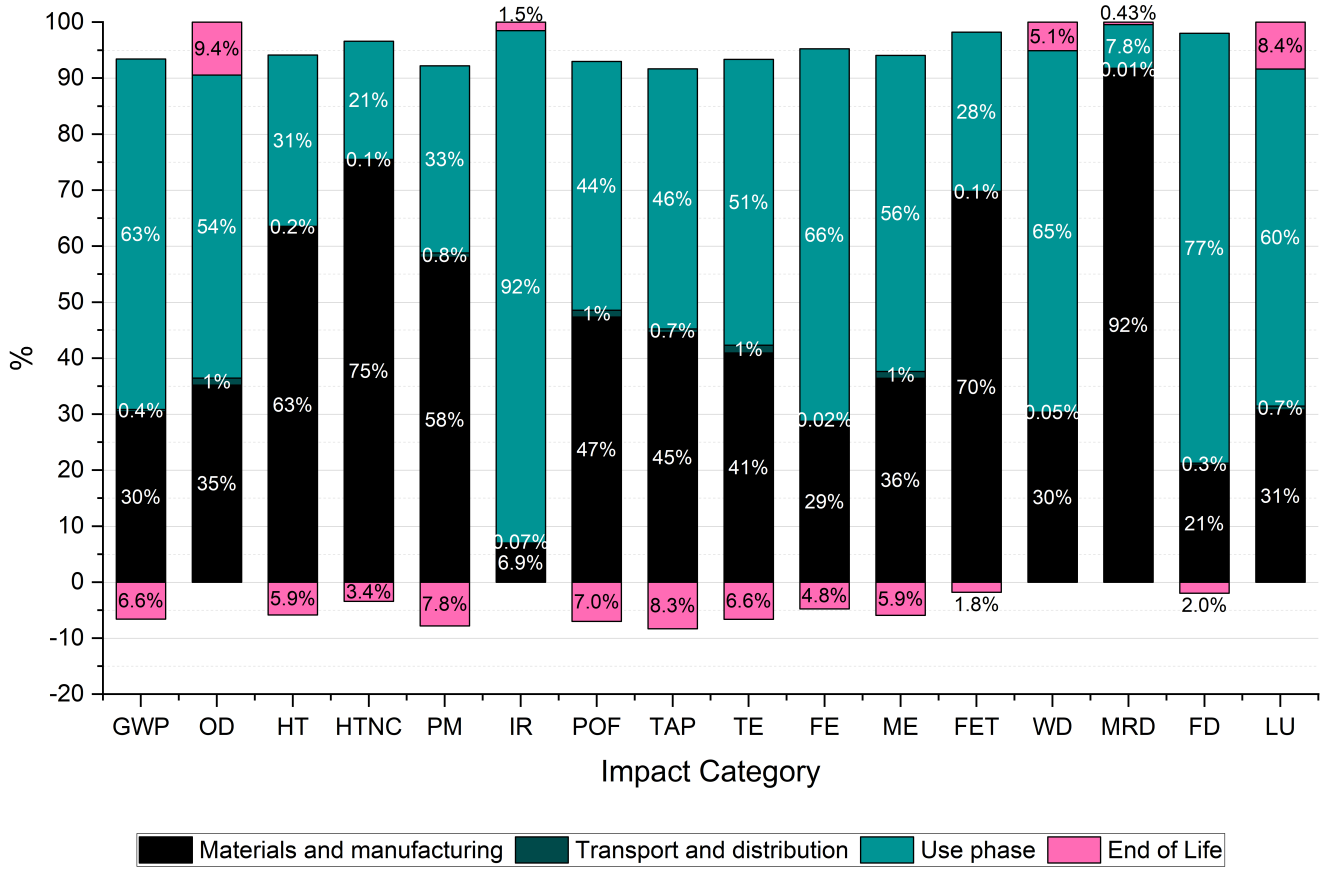


FIGURE 3. LCA results of the case study by life cycle phases percentage contribution. ***Materials and manufacturing*** includes raw material extraction, component production, and inverter manufacturing/assembly. ***Transport and distribution*** includes the transport of individual components, such as the power module, DC-link, mechanical parts and bus bars, as well as the final distribution of the inverter. ***Use phase*** accounts for the environmental impact associated with the energy consumed during inverter operation. ***End of Life*** includes the treatment, recycling, recovery, or disposal processes at the end of the inverter lifetime.

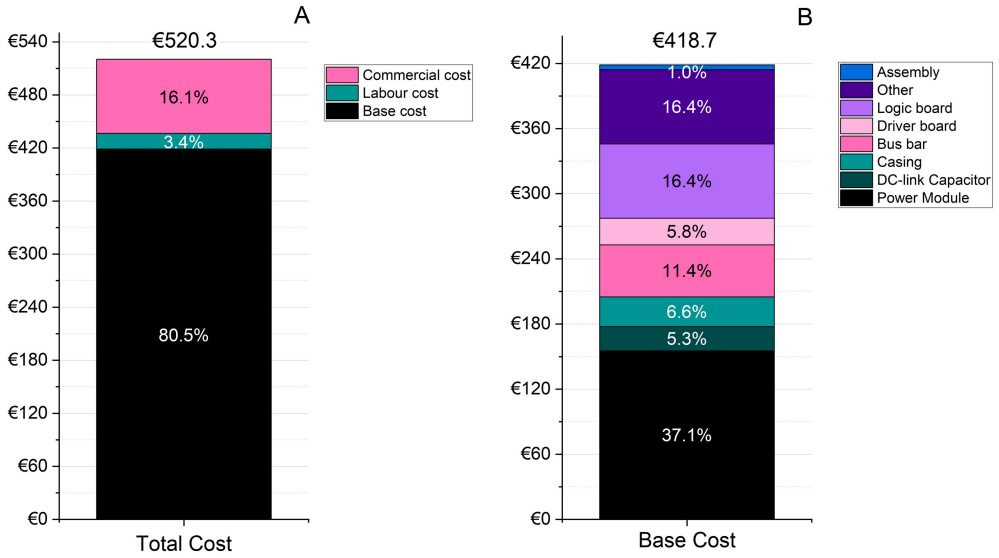


FIGURE 4. LCC of the case study shown as: A: total cost breakdown by cost category; B: base cost breakdown by inverter components.

While silicon-based power devices continue to advance, they are approaching their fundamental performance limits because of the intrinsic properties of silicon, including its relatively low bandgap, critical electric field, and thermal

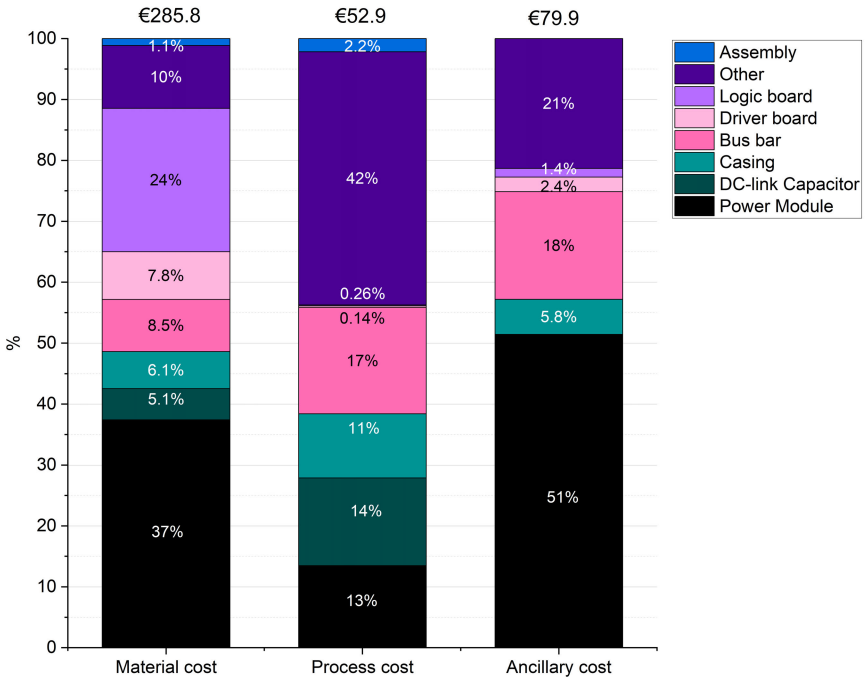


FIGURE 5. Base cost breakdown for the case study, by cost source (material costs, process costs and ancillary costs).

conductivity. These limitations result in higher conduction and switching losses as well as reduced performance at elevated temperatures [67]. In this context, silicon carbide (SiC) technology offers a promising alternative. Although SiC devices typically cost two to three times more than their silicon counterparts, their higher efficiency and ability to operate at higher switching frequencies enable reductions in passive-component requirements and cooling-system complexity, ultimately lowering the overall system cost according to [67].

Figure 5 presents a detailed breakdown of the base cost, both in absolute terms and as percentages, highlighting the contributions of each cost category: material cost, process cost, and ancillary cost. The power module emerges as the primary hotspot, accounting for 37% of raw material costs and 51% of ancillary costs. The latter is attributed to the consumption of alumina substrate and potassium hydroxide in the DCB. Additionally, the category labeled "other" constitutes another significant hotspot, contributing 42%, primarily due to the process cost associated with plated cable glands. The cost of the logic board, contributing 24%, is predominantly influenced by the materials employed.

B. MODEL VALIDATION

Since both the LCA and LCC models rely on the scaling methodology proposed by [41], a multi-step validation procedure was carried out to assess the robustness of the proposed framework. This section comprises three validation levels.

First, the inverter masses estimated through the scaling methodology were validated against available reference data to evaluate the reliability of the inventory generation process and the resulting LCI. This step aimed to verify the capability of the scaling approach to accurately reproduce the physical characteristics of the inverter (Section III-B1).

Subsequently, both the environmental and economic results were validated against external sources using the most appropriate reference data available for each domain. For the environmental assessment, direct measurement data are generally not available; therefore, the LCA results were benchmarked against those reported in the literature, specifically the study by [20] (Section III-B2). In contrast, the economic results can be compared with observable market values. Consequently, the LCC results were validated against inverter cost estimates available for several electric vehicle models to assess the reliability of the scaling approach (Section III-B3).

1) MASS VALIDATION AGAINST REFERENCE DATA

Figure 6 shows the inverter masses expressed as a function of power (kW) and voltage (V). The inverter masses derived from the model generate limit curves that define the models area of validity. The area boundaries correspond to 250 V (minimum, purple) and 700 V (maximum, green). Real inverter data (black and red scatters) were then positioned against this cone, distinguishing between semiconductor technologies used: IGBT inverters are shown with red scatter points, while other inverters (SiC and GaN) are depicted with black scatter points.

This validation step revealed that the model tends to overestimate the mass of inverters compared to real systems. For instance, the commercial inverter installed in the VW ID.4 RWD has a total weight of about 8–10 kg, while the model estimated 14.9 kg. Similar discrepancies were found for other inverters used in different electric vehicles. In fact, the red scatters consistently lie below the limit curves, confirming the models tendency to overestimate the inverter mass. Moreover, the presence of high-power and high-voltage inverters (above 150 kW and up to 800 V) as well as technologies beyond IGBT (e.g., SiC-MOSFET or GaN-MOSFET) highlight the need for further refinement and potential revision of the scaling methodology. This deviation is systematic rather than random, as all the real inverters collected lie below the limit curves of the model, and it is consistent with the vintage of the reference data underlying [41], which describe components released between 2008 and 2014 against a case study designed in 2020. A further contribution arises from the casing, modelled as a stand-alone die-cast enclosure with a wall thickness derived from expert judgement and identified by its authors as the subpart affected by the largest uncertainty, whereas in the reference vehicle the inverter is integrated in the rear e-axle and shares housing and cooling circuit with the electric machine.

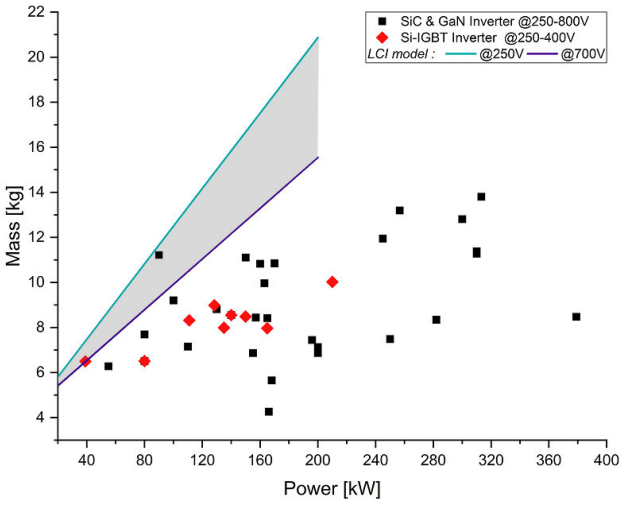


FIGURE 6. Real inverters (black and red scatters) and the model's area of validity as a function of voltage and power. Area boundaries correspond to 250 V (minimum, purple) and 700 V (maximum, green).

The additional datasets enabled the application of a statistical adjustment to investigate whether a better trend of mass as a function of power and voltage could be identified, and to evaluate whether the model could be reconfigured and better aligned with real-world values. Focusing on IGBT-based systems up to 400V, a first tentative correction trend line was derived, with a coefficient of determination of approximately 0.75. Once this trend line was established, additional IGBT-based inverters (blue stars) were identified to validate the corrected model. Using the first group of samples, a linear regression model was developed to describe the relationship between inverter mass and rated power. The resulting correlation is expressed by:

$$y = 5.60 + 0.020 \cdot x \tag{7}$$

where (y) represents the inverter mass and (x) the rated power. The fitted model achieved a coefficient of determination (R^2) of 0.75, indicating that a substantial proportion of the variability in inverter mass is explained by the rated power. Furthermore, the regression coefficient associated with power was $p = 0.0023$ (statistically significant), with a 95% confidence interval ranging from 0.0098 to 0.0298. Since the interval lies entirely above zero, the results confirm a positive relationship between rated power and inverter mass. The root mean square error is 0.59 kg that can be regarded as relatively small, considering that the inverter masses in the dataset range between 6 and 10 kg. This suggests that the regression provides an adequate representation of the data and satisfactory predictive performance within the investigated voltage range.

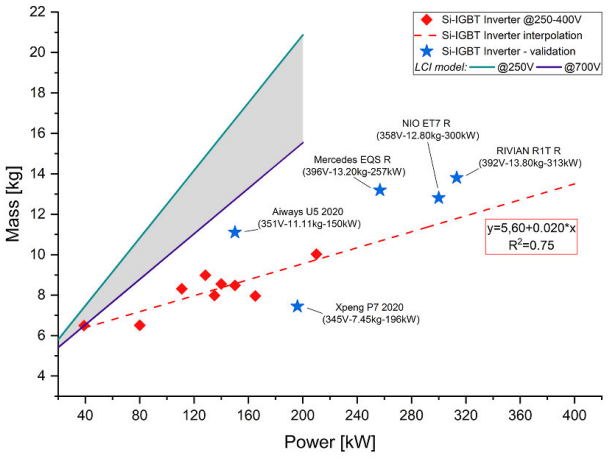


FIGURE 7. Real IGBT inverters (red scatters), validation samples (blue stars) and the model's cone of validity as a function of voltage and power. Corrected mass trend in dashed red.

It should be noted that the available dataset only included inverters used in vehicles with onboard voltages up to 400 V, limiting the validation of the regression model to the 250-400 V voltage range. Nevertheless, this represents a solid starting point for an LCI scaling approach. Previous studies have shown that the mass of electrical and electronic components, such as cables, generally decreases as system voltage increases [68]. Consequently, it is reasonable to expect a weaker dependence of inverter mass on rated power at higher voltage levels, resulting in a lower slope of the mass–power relationship. This hypothesis is consistent with the trends predicted by the implemented model (Figure 7).

Within this domain, Eq. 7 can be applied to a broad range of current battery electric passenger vehicles. Its use outside this domain is not recommended for the following reasons: (a) 800 V architectures are not covered, as no unit

with a DC-link voltage above 400 V was available in the dataset; since the mass of the conductive parts decreases with increasing voltage at constant power [67], the slope of the mass–power relationship is expected to be lower at 800 V, and Eq. 7 would consequently overestimate the mass; (b) wide-bandgap devices, as SiC and GaN units achieve higher gravimetric power densities and lie systematically below the fitted correlation, as visible in Figure 6; (c) integrated e-axle units, where the inverter shares housing and cooling with the electric motor, making the mass attributable to the inverter dependent on the allocation criterion adopted and therefore not directly comparable with that of a stand-alone unit; (d) non-automotive and air-cooled applications, which are characterised by different packaging and thermal management constraints.

2) LCA VALIDATION AGAINST THE LITERATURE

To validate the model against a comparable LCA study from the literature, the same input parameters adopted by [20] were used, namely an inverter rated at 150 kW and 450 V. Specifically, the simulations were performed under the same operating conditions reported in the reference study, namely the same LCIA EF3.0 method and background Ecoinvent database. The comparison across the impact categories shows that the relative percentage errors between the model outputs and the results reported by [20] are generally low (Table 4), indicating good agreement between the two studies. Nevertheless, larger deviations were observed for some impact categories: non-cancer human toxicity, cancer human toxicity, acidification, freshwater eutrophication, freshwater ecotoxicity, water use, resource use of minerals and metals and land use.

TABLE 4. Comparison of model results with [20].

Impact Category	Model	Reference	Error %
Climate change	3.22E+02	3.42E+02	5.95%
Ozone depletion	2.33E-05	2.14E-05	8.84%
Human toxicity, cancer	5.41E-07	2.14E-05	97.5%
Human toxicity, non-cancer	2.63E-05	1.72E-04	84.7%
Particulate matter	2.35E-05	2.23E-05	5.15%
Ionising radiation	2.24E+01	2.24E+01	0.10%
Photochemical ozone formation	1.38E+00	1.57E+00	12.3%
Acidification	3.29E+00	2.46E+00	33.34%
Eutrophication, terrestrial	4.37E+00	4.91E+00	10.9%
Eutrophication, freshwater	2.59E-01	3.29E-01	21.1%
Eutrophication, marine	4.07E-01	4.47E-01	8.99%
Ecotoxicity, freshwater	2.35E+04	6.80E+02	3363%
Water use	8.26E+01	1.15E+02	28.3%
Resource use, minerals & metals	5.09E-02	7.58E-02	32.8%
Resource use, fossils	3.59E+03	3.75E+03	4.22%
Land use	1.33E+03	2.44E+03	45.5%

Figure 8 shows the comparison between the LCIA results obtained from the developed model and those reported in the reference study. The aim of this analysis was to assess whether the environmental impacts attributed to the individual inverter components were consistent across the two studies, both in terms of magnitude and relative contribution to each impact category.

For most impact categories, the agreement between the two sets of results was considered satisfactory. As shown in Figure 8, the climate change (GWP) category exhibits comparable impact magnitudes for the power module, DC-link capacitor, and other inverter components. Moreover, the casing is identified as the dominant contributor in both studies, indicating a consistent distribution of impacts among components. Similar observations can be made for the ozone depletion (OD) and ionizing radiation (IR) categories.

Finally, for the categories previously identified as the most divergent, both the orders of magnitude and the percentage distribution of components show significant discrepancies between the two studies (Figure 9). For instance, in the case of the bus bars, a considerable difference was observed between the developed model and the reference study, resulting in a greater impact in this study compared to the literature reference. Differences in the component contributions were also observed for the resource use of minerals and metals (MRD). For example, power modules have less impact in this study compared to the literature reference. These discrepancies in the impact categories can be attributed to the use of different database versions and selected datasets between the present and the reference study.

3) COST VALIDATION AGAINST BENCHMARK DATA

Continuing with the cost model analysis, the cradle-to-gate total cost was evaluated and compared with other benchmark analysis. Figure 10 shows this comparison revealing a consistent upward trend of costs with increasing power for both. This indicates that the constructed model and the real data are comparable, as they exhibit similar behavior.

It should be noted that the developed LCC model (purple curve) tends to yield higher cost estimates than those reported in other benchmark studies (magenta points). To quantify this discrepancy, the model predictions were compared with the available reference values by calculating the mean relative interpolation error, which was found to be 16.5%. Despite this divergency, the result can be considered acceptable, as the regression line remains within the distribution of validation samples represented by the benchmark data. This indicates that the model is able to capture the overall cost trend with a reasonable level of accuracy. For the case study considered, the LCC model predicts an inverter cost of €520, whereas benchmark analyses report values of approximately €400.

C. DESIGN IMPLICATIONS AND ECO-DESIGN GUIDELINES

The combined reading of the environmental and economic results allows a set of design indications to be derived for each of the main subcomponents of the inverter. Because both assessments are built on the same inventory, the levers identified below can be evaluated simultaneously against the two dimensions, and in several cases the two point in different directions.

The aluminium casing, which accounts for 44% of the cradle-to-gate GWP, is affected almost entirely by upstream,

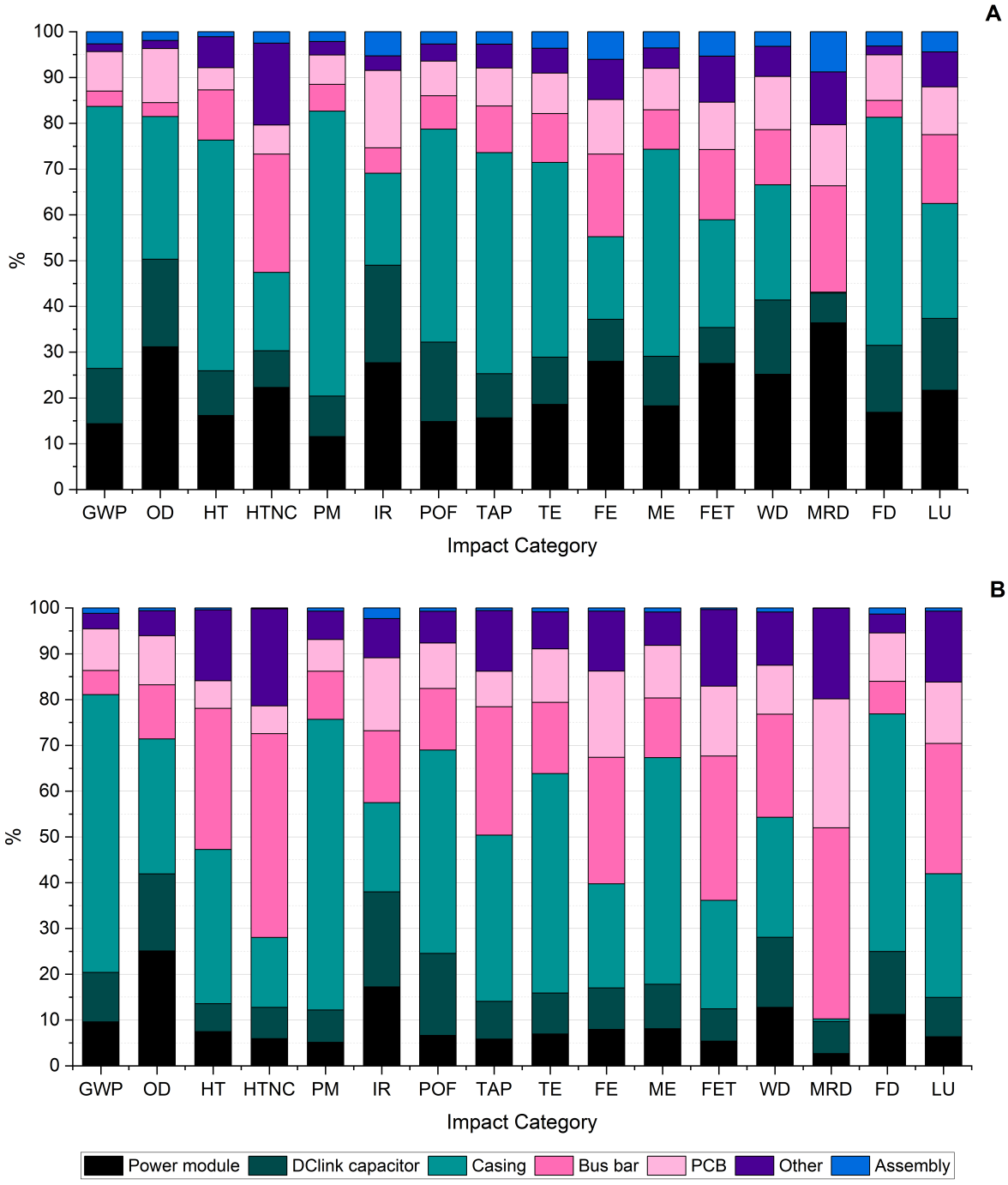


FIGURE 8. Environmental breakdown comparison between (A) results from [20] and (B) results obtained by running the LCA-LCC model with the same input parameters as in [20].

electricity-driven processes, since primary aluminium is modelled with the RoW mix. Three levers are available, in increasing order of effectiveness. The first is the sourcing of primary aluminium from low-carbon smelters, such as the hydro-based European supply, or, more effectively, the adoption of secondary aluminium, which reduces the cradle-to-gate GWP of the material by approximately one order of magnitude [51], [52]. The second is the reduction of mass through the optimisation of the wall thickness of the die-cast housing. The third is the structural integration of the inverter housing into the e-axle or gearbox housing, which removes the need for a dedicated enclosure and for part of the cooling interface. Since the casing accounts for only 6.6% of the base cost, these measures are environmentally effective at a limited



FIGURE 9. Environmental breakdown comparison between (A) literature results based on [20] and (B) results obtained by running the LCA-LCC model with the same input parameters as in [20]. Focus on the most divergent impact categories: non-cancer human toxicity, cancer human toxicity, acidification, freshwater eutrophication, freshwater ecotoxicity, water use, resource use of minerals and metals and land use.

economic penalty, which is a direct outcome of the integrated assessment.

The DC-link capacitor, responsible for 30% of the cradle-to-gate GWP, is sized by the admissible voltage ripple and by the ripple current. Higher switching frequencies, enabled by wide-bandgap devices, together with interleaving and improved modulation strategies, reduce the required capacitance and therefore the embedded impact, while increasing the DC-link voltage at constant power reduces the current and further relaxes the requirement. Ceramic DC-link solutions [35] represent an alternative with a different impact profile, whose assessment is indicated as a direction for future work.

Bus bars and conductive parts, which dominate human toxicity, acidification, freshwater eutrophication and ecotoxicity, and the use of mineral and metal resources, are governed by copper production. The available levers are the increase of the system voltage, since an 800 V architecture halves the current and therefore the required conductor cross-section at equal power [68], the substitution of copper with aluminium

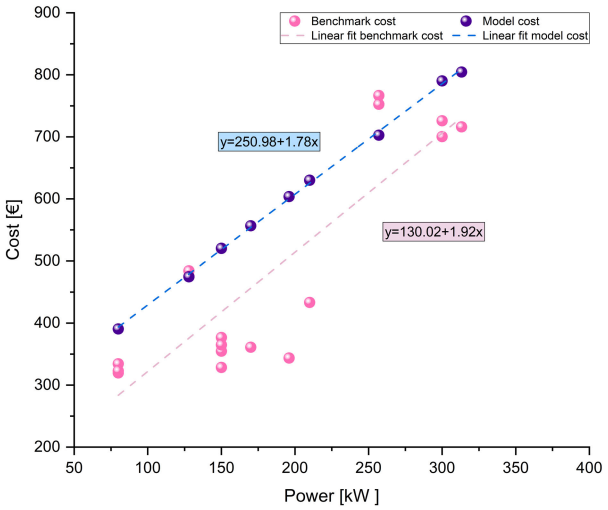


FIGURE 10. IGBT inverter cradle-to-gate total costs obtained with the model (purple points) and benchmark costs (magenta points) with corresponding interpolating trends.

wherever the admissible current density and the joining technology allow it, and the adoption of recycled copper content.

The power module, which represents 37.1% of the base cost and 51% of the ancillary cost while exceeding 10% of ozone depletion, ionising radiation and mineral and metal resource use, requires distinct actions on the two dimensions. On the economic side, cost reduction must act on the die area, that is on the utilisation of the silicon, and on the packaging: reverse-conducting and reverse-blocking architectures [65] reduce module volume and weight, while integrated liquid-cooled modules remove a mechanical interface. On the environmental side, the contributions to ozone depletion and ionising radiation originate from wafer fabrication, with 76% and 63% respectively, and are therefore reduced by any measure that decreases the active silicon area, whereas the use of mineral and metal resources is dominated by the antimony contained in lid and frame, with 67%, which points to material substitution in the package as a specific and actionable recommendation.

The use phase, which accounts for 63% of the cradle-to-grave GWP and exceeds 70% of ionising radiation and fossil resource use, confirms conversion efficiency as the single most effective environmental lever at vehicle level, since the impact associated with the operating losses exceeds the entire embodied impact of the inverter by a factor of about two. This establishes a quantifiable eco-design trade-off: a technology characterised by a higher embodied impact but by a higher conversion efficiency, such as a silicon carbide solution, is environmentally advantageous provided that the additional embodied burden is repaid by the reduction of the losses accumulated over the lifetime of the component.

Finally, since the assembly stage is electricity-intensive, the carbon intensity of the electricity supplied to the manufacturing site constitutes a further lever, of direct relevance to the site-selection decisions of component suppliers.

D. SENSITIVITY ANALYSIS

The validation steps described above showed that the scaling methodology tends to overestimate the inverter mass. To assess how such an inaccuracy would propagate to the results, a sensitivity analysis was performed following the one-at-a-time (OAT) approach also adopted in [20]. The mass of a single component was reduced by 10% while all the remaining components were held at their baseline value, and the environmental and economic indicators were recomputed on the resulting inventory. The procedure was repeated for the four components identified as environmental or cost hotspots in Figures 2 and 4, namely the power module, the aluminium casing, the DC-link capacitor and the laminated bus bar. Since both models are implemented on the same inventory within a single project, the environmental and the economic sensitivities are directly comparable.

Depending on the share that each component represents of the complete unit, a 10% reduction of its mass corresponds to a variation of the total inverter mass between 0.87% and 4.71%. Table 5 shows the resulting change in the sixteen impact categories for each of the four sensitivity scenarios, whilst Table 6 reports the variation of the life cycle cost.

The environmental response is bounded: no impact category varies by more than 5.2% in any of the four scenarios, the largest effect being observed on non-cancer human toxicity for the bus bar. The analysis also shows that the environmental profile is not governed by a single component. The laminated bus bar produces the largest variation in seven impact categories, mainly those associated with metal production, namely human toxicity with and without cancer, freshwater ecotoxicity, freshwater eutrophication, acidification, land use and resource use of minerals and metals. The DC-link capacitor leads in five categories, including ozone depletion, ionising radiation and photochemical ozone formation. The aluminium casing leads in four, including climate change and particulate matter, which are dominated by the electricity-intensive production of primary aluminium. The power module does not lead in any impact category, its largest effect being a 2.4% variation of mineral and metal resource use, since its environmental profile is governed by a few grams of critical substances and by the active die area rather than by its bulk material.

The economic response follows a different order. The power module governs the cost sensitivity with a 3.81% variation of the total life cycle cost, more than four times the effect of the aluminium casing, which produces only 0.87% despite representing a considerably larger share of the inverter mass. The laminated bus bar and the DC-link capacitor lie in between, at 1.33% and 0.75% respectively. When the variations are normalised by the corresponding change of the total inverter mass, the divergence becomes explicit: the power module returns 2.70 percentage points of cost reduction per percentage point of mass removed, against

TABLE 5. Variation of the environmental indicators for a 10% reduction of the mass of each hotspot component. Each column corresponds to an independent sensitivity scenario in which only the indicated component is varied. The largest variation in each category is highlighted in green.

Impact category	Unit	Sensitivity scenario			
		Power module sensitivity	Casing sensitivity	DC-link capacitor sensitivity	Laminated bus bar sensitivity
Climate change	kg CO_2 eq	−1.13%	−4.64%	−3.22%	−0.95%
Ozone depletion	kg CFC11 eq	−2.11%	−2.07%	−4.20%	−1.51%
Ionising radiation	kBq U-235 eq	−1.52%	−1.33%	−4.67%	−1.87%
Photochemical ozone formation	kg NMVOC eq	−0.86%	−2.91%	−4.34%	−1.74%
Particulate matter	disease inc.	−0.84%	−5.04%	−2.28%	−1.71%
Human toxicity, non-cancer	CTUh	−1.09%	−1.16%	−1.80%	−5.20%
Human toxicity, cancer	CTUh	−1.18%	−2.47%	−1.77%	−4.03%
Acidification	mol H^+ eq	−0.99%	−2.60%	−2.28%	−3.62%
Eutrophication, freshwater	kg P eq	−1.15%	−1.70%	−2.44%	−3.52%
Eutrophication, marine	kg N eq	−1.07%	−3.71%	−2.83%	−1.93%
Eutrophication, terrestrial	mol N eq	−1.01%	−3.59%	−2.62%	−2.26%
Ecotoxicity, freshwater	CTUe	−1.04%	−1.77%	−1.98%	−4.02%
Land use	Pt	−1.04%	−1.98%	−2.33%	−3.64%
Water use	m^3 depriv.	−1.44%	−1.80%	−3.67%	−2.72%
Resource use, fossils	MJ	−1.22%	−3.74%	−3.75%	−1.13%
Resource use, minerals and metals	kg Sb eq	−2.40%	−0.27%	−1.60%	−4.19%

0.18 for the casing, while the bus bar returns 3.16 percentage points of average environmental reduction, against 0.54 for the casing. Mass is therefore not a proxy for either the environmental or the economic performance, and the two optimisation directions do not act on the same component.

Two conclusions can be drawn. First, the model is robust with respect to inventory inaccuracies of the order investigated: an error of 10% on any single hotspot changes every environmental indicator by less than 5.2% and the total cost by less than 3.9%, without reversing the hierarchy of the contributions or altering the eco-design indications derived from the case study. Second, the analysis provides a quantitative ranking of the design levers, in which the laminated bus bar emerges as the most efficient joint target, being the leading contributor in seven impact categories and the second economic lever while representing a minor share of the inverter mass.

TABLE 6. Variation of the life cycle cost for a 10% reduction of the mass of each hotspot component. Each row corresponds to an independent sensitivity scenario in which only the indicated component is varied.

Sensitivity scenario	Base cost	Total cost
Power module scenario	−3.94%	−3.81%
Laminated bus bar scenario	−1.38%	−1.33%
Aluminium casing scenario	−0.90%	−0.87%
DC-link capacitor scenario	−0.77%	−0.75%

IV. CONCLUSION

The study provided an in-depth overview of the environmental and economic sustainability of automotive IGBT inverters. The research has shown that LCA is a robust tool to evaluate such impacts and to assess whether next-generation electric vehicles can truly be considered a sustainable alternative. The results indicate that even the production of the inverter entails significant environmental burdens, both for ecosystems and for human health. In particular, the DC-link capacitor, the aluminum casing, and the bus bars proved to be the most impactful subcomponents. The analysis further revealed that copper-related processes play a significant role in the environmental footprint, especially in components like bus bars. This is relevant, as copper is widely used across the multiple electronic subsystems of electric vehicles. Nonetheless, higher operating voltages could reduce the amount of conductive material required, thereby lowering copper-related impacts. This underlines the importance of including production processes and the associated energy mix when comparing electric vehicles with internal combustion engine vehicles.

From the LCC perspective, results showed that the power module is the most cost-intensive part of the inverter. This is reasonable given the large number of components it integrates, many of which involve precious metals, complex processes, and auxiliary substances. Again, the increase in voltage levels may help reduce the required mass of conductive materials, potentially lowering costs.

The practical relevance of the integrated approach is demonstrated by a key finding: the environmental and economic hotspots of the same product do not coincide. The aluminium casing and the DC-link capacitor dominate the cradle-to-gate GWP (44% and 30%, respectively), whereas the power module accounts for 37.1% of the base cost while contributing only 8.9% of the GWP. A purely environmental or purely techno-economic study would therefore point to opposite design priorities, a trade-off that can only be identified through a jointly constructed assessment.

Regarding the limitations of this study, cost overestimations in the model were likely due to mass overestimations identified during the analysis. The first tentative refinement of the mass estimation highlighted how inverter technology has evolved over time, not only functionally but also in terms of design and materials. For instance, components such as high-voltage connectors increasingly employ plastics and complex geometries, changing both processes and costs, in line with the widespread adoption of electric vehicles.

To quantify the consequences of such an inaccuracy on the results, a one-at-a-time sensitivity analysis was performed by reducing by 10% the inventory of each hotspot component. The results showed that an inaccuracy of this order changes every environmental indicator by less than 5.2% and the total life cycle cost by less than 3.9%, without altering the hierarchy of the contributions. The analysis further highlighted that the environmental and the economic sensitivities are governed by different components, the casing and the bus bar on the environmental side and the power module on the economic one, and that the laminated bus bar represents the most efficient joint target for eco-design, since it leads in seven impact categories and is the second economic lever while accounting for a minor share of the inverter mass.

A further limitation concerns the temporal validity of the economic results, since the cost figures presented in this work are representative of market conditions as of 2025. Given the volatility of commodity prices and the rapid evolution of the semiconductor market, the absolute cost figures should be interpreted with caution beyond a horizon of approximately two to three years. The component ranking and the identification of the cost hotspots, however, are expected to remain valid over a longer period, as they are governed by the architecture of the product rather than by market conditions.

Future improvements should involve collecting more detailed data on individual components to refine mass estimates and improve the model, currently valid only for up to 400 V IGBT inverters. Alongside IGBTs, alternatives such as MOSFETs based on silicon carbide (SiC) or gallium nitride (GaN) are emerging. These materials are increasingly relevant as the automotive sector moves toward higher voltage and higher power architectures. They offer greater efficiency, the ability to operate at higher frequencies, and improved thermal resilience, which are key requirements for sustainable mobility. While these technologies were once deemed too expensive, the trend is shifting as the industry prioritizes fast charging, higher voltage systems, and sustainability. This transition could redefine the role of electric vehicles, reinforcing their potential to replace internal combustion vehicles as the predominant means of global transport. Looking forward, applying combined LCA/LCC methodologies to SiC and GaN-based inverters would provide valuable insights.

Lastly, future works should consider the inclusion of recycled materials in the manufacturing processes. In fact, circular economy application in electronics, would allow materials that would otherwise be discarded to be reused, reducing economic, social, and environmental impacts, as well as health risks [69].

APPENDIX A
COST MODEL INSIGHT

A. MATERIAL COST

The material cost category C_{mat} includes all primary materials that make up the inverter. Specifically, this refers to both the inverter subcomponents and the input materials that directly form the inverter unit. The former mainly consists of electronic subsystems (e.g., diodes, resistors, or connectors), while the latter includes raw materials (e.g., copper, brass, polymers) that may undergo processing or be used directly as sealants or insulators. The construction of this portion of the raw material cost database was based mainly on metal stock market indices, including ferrous alloys (e.g., steel) and non-ferrous alloys (e.g., aluminum) [70], [71], [72], [73]. For some materials, a portion of the alloy was assumed to be sourced from recycled content. For example, brass was selected because it is fully recyclable and well suited for electronic applications [74]. The final material cost was estimated assuming a recycled content of 50%, calculated as the average of the price of virgin brass (approximately €8/kg) [70] and the price of recycled brass available through scrap metal trading platforms (approximately €2–3/kg) [75]. Electronic component costs were selected from catalogs of various international suppliers or based on cost studies from the literature.

B. ANCILLARY COST

The ancillary cost category C_{anc} includes components, reagents, or disposables used in the inverter manufacturing process that are not intended to be part of the final product. However, they play a decisive role in all secondary or auxiliary processes during manufacturing [76], and can significantly affect the final cost. Examples include lubricant oils or chemicals used for washing and rinsing processes. Unit costs have been identified through the literature research. The application of quantity discounts was challenging in this case and was not always possible due to the high variability of the data. For deionized water, the unit cost in €/kg was determined using the lowest market price and applying a quantity discount of 30% reflecting industrial-scale usage rather than retail or laboratory prices [77]. This approach ensures representative costs for high-volume production.

C. PROCESS COST

The process cost category C_{proc} refers to the costs arising from manufacturing processes. These costs were found to be

significant during the study. Various mechanical processes are involved in the production of the inverter, including metalworking and operations on secondary parts made of plastics or polymers. Unit process costs were determined using the literature [78], company reports [79], specialized websites [80], and available primary data. For processes with missing cost data, specialized cost engineering software was used, inputting reasonable cycle times and operator numbers to obtain unit process costs. For example, copper sheet rolling was assumed to take a 10-second cycle per kg, with one operator, yielding a process cost of 0.3 €/kg.

APPENDIX B
PARAMETRIZATION INSIGHT

The parameterisation follows the scalable inventory of Nordelöf and Alatalo [41] and is implemented in SimaPro as a set of parametric expressions driven by two user inputs, the rated power P and the DC-link voltage V. The model estimates the maximum operating condition as $P_{\max} = 1.5P$ and $V_{\text{cut-off}} = 0.75V$, i.e. peak power at the minimum battery voltage, and scales each macro-component through the quantity identified in [41] as its dominant driver.

- **Power module:** the mass of each constituent (copper of baseplate, DCB foils, bond wires and terminals; alumina substrate; doped silicon; solder; PPS and glass-fibre frame; silicone gel; nickel, gold and zinc coatings) is obtained by linear interpolation between two reference modules rated 20 kW and 80 kW, $m_s = m_s(20\,\text{kW}) + k_s(P - 20)$, with the coefficients k_s reported in Table 1 of [41]. The active die area used for the wafer input is derived from the scaled mass of doped silicon ($5.92\,\text{cm}^2\,\text{g}^{-1}$). The module is a function of power only.
- **DC-link capacitor:** ripple-current handling is the sizing criterion, and it leads to a capacitance, and hence a mass, proportional to P/V. The mass is therefore obtained as $m = k_c P/V$, with $k_c = 7.14\,\text{g V kW}^{-1}$ fitted on four commercial metallised-film automotive capacitors rated 450 V (15–$17.5\,\text{g kW}^{-1}$); the material composition is kept constant over the whole domain.
- **Laminated bus bar:** the maximum DC and AC currents are computed as $I_{\text{DC}} = P_{\max}/(\eta V_{\text{cut-off}})$ and $I_{\text{AC}} \approx P_{\max}/V_{\text{cut-off}}$, the conductor cross-sections from an admissible current density of $5\,\text{A mm}^{-2}$ ($0.2\,\text{mm}^2\,\text{A}^{-1}$) with a 5% allowance per additional layer, and the conductor lengths by linear scaling ($1.2\,\text{mm kW}^{-1}$ on the DC side, $0.8\,\text{mm kW}^{-1}$ on the AC side); the copper mass follows from length, cross-section and density.
- **Casing:** the housing compartment and the liquid-cooled heatsink are scaled linearly from the reference units, $1.70\,\text{kg} + 10.2\,\text{g kW}^{-1}$ and $2.10\,\text{kg} + 13.6\,\text{g kW}^{-1}$ respectively, the heatsink reference design being sized in [41] for continuous operation at 150% of the rated power. The thermal interface material is scaled through the mounting surface, assuming a 100 μm layer.
- **Logic and driver boards:** both are modelled as constant over the whole domain ($1.5\,\text{dm}^2$ and $0.7\,\text{dm}^2$ respectively), since [41] found no correlation between board size or component count and rated power, the mass difference over the 20–200 kW span being of the order of 5 g.
- **Ancillary materials, process times and energy consumption** are scaled through the derived geometrical quantities (plated and anodised surfaces, DCB and baseplate areas, soldered board area) rather than through mass.

The validity domain of the parameterisation is 20–200 kW and 250–700 V. It should be noted that the voltage input affects only the DC-link capacitor mass and the bus bar cross-sections; all other macro-components are scaled through power alone, which explains the limited width of the model validity region in Figure 6.

ACKNOWLEDGMENT

This work was performed at the Interdepartmental Center for Automotive Research and Sustainable mobility (CARS) at Polytechnic of Turin. Views and opinions expressed are, however, those of the author(s) only and do not necessarily reflect those of European Union or European Climate, Infrastructure and Environment Executive Agency (CINEA). Neither the European Union nor CINEA can be held responsible for them.

REFERENCES

[1] S. Kara, W. Li, and N. Sadjiva, "Life cycle cost analysis of electrical vehicles in Australia," *Proc. CIRP*, vol. 61, pp. 767–772, Jan. 2017. [Online]. Available: https://www.sciencedirect.com/science/article/pii/S2212827116313397

[2] M. Räikkönen, L. Sokka, L. Hepo-oja, S. Nordman, and T. M. Kraft, "Sustainable production insight through LCA and LCC analysis of injection overmolded structural electronics manufactured through Roll-to-Roll processes," *Global Challenges*, vol. 7, no. 11, Nov. 2023, Art. no. 2300015. [Online]. Available: https://onlinelibrary.wiley.com/doi/abs/10.1002/gch2.202300015

[3] A. Kampker, H. Born, M. Nankemann, and J. Wollgarten, "Qualitative study on the use of life cycle assessments in electric drive production," in *Proc. 14th Int. Electr. Drives Prod. Conf. (EDPC)*, Nov. 2024, pp. 1–6. [Online]. Available: https://ieeexplore.ieee.org/document/10932850/

[4] W. Kloepffer, "Life cycle sustainability assessment of products: (with comments by helias A. Udo de haes, p. 95)," *Int. J. Life Cycle Assessment*, vol. 13, no. 2, pp. 89–95, Mar. 2008. [Online]. Available: http://link.springer.com/10.1065/lca2008.02.376

[5] S. Lazzari and A. Levizzari, "Life cycle costing as a new tool matching economical and environmental evaluations: The experience on a real case study," *Total Life Cycle Conf. Expo.*, Detroit, MI, USA, Apr. 2000. [Online]. Available: https://doi-org.ezproxy.biblio.polito.it/10.4271/2000-01-1466

[6] G. Norman, "Life cycle costing," *Sustainability Assessment Renewables-Based Products*, vol. 8, no. 4, pp. 344–356, 1990. [Online]. Available: https://onlinelibrary.wiley.com/doi/pdf/10.1002/9781118933916.ch14.

[7] F. Testa, F. Iraldo, M. Frey, and R. O'Connor, "Life cycle costing, a view of potential applications: From cost management tool to eco-efficiency measurement," *Supply Chain Manag.*, pp. 569–590, Apr. 2011. [Online]. Available: https://www.intechopen.com/chapters/15555

[8] A. Luthin, J. G. Backes, and M. Traverso, "A framework to identify environmental-economic trade-offs by combining life cycle assessment and life cycle costing—A case study of aluminium production," *J. Cleaner Prod.*, vol. 321, Oct. 2021, Art. no. 128902. [Online]. Available: https://linkinghub.elsevier.com/retrieve/pii/S0959652621030961

[9] K. Lu, X. Jiang, J. Yu, V. W. Y. Tam, and M. Skitmore, "Integration of life cycle assessment and life cycle cost using building information modeling: A critical review," *J. Cleaner Prod.*, vol. 285, Feb. 2021, Art. no. 125438. [Online]. Available: https://www.sciencedirect.com/science/article/pii/S0959652620354846

[10] P. Schneider-Marin, A. Winkelkotte, and W. Lang, "Integrating environmental and economic perspectives in building design," *Sustainability*, vol. 14, no. 8, p. 4637, Apr. 2022. [Online]. Available: https://www.mdpi.com/2071-1050/14/8/4637

[11] M. Kalverkamp, E. Helmers, and A. Pehlken, "Impacts of life cycle inventory databases on life cycle assessments: A review by means of a drivetrain case study," *J. Cleaner Prod.*, vol. 269, Oct. 2020, Art. no. 121329. [Online]. Available: https://www.sciencedirect.com/science/article/pii/S0959652620313767

[12] G. K. Booto, K. A. Espegren, and R. Hancke, "Comparative life cycle assessment of heavy-duty drivetrains: A Norwegian study case," *Transp. Res. D, Transp. Environ.*, vol. 95, Jun. 2021, Art. no. 102836. [Online]. Available: https://www.sciencedirect.com/science/article/pii/S1361920921001395

[13] Y. Nakamura, A. Yamaguchi, R. Ishido, J. Kashiwagi, Y. Oku, and K. Nakahara, "Model-based cost-benefit analysis on Si/SiC hybrid switches for traction inverters," in *Proc. PCIM Conf. Int. Exhib. Conf. Power Electron., Intell. Motion, Renew. Energy Energy Manag.*, May 2025, pp. 2683–2687. [Online]. Available: https://ieeexplore.ieee.org/document/11053641/

[14] M. Walter and M.-M. Bakran, "Hybrid-switch-inverter—A new approach reducing the system cost of the electric powertrain," in *Proc. PCIM Eur. Int. Exhib. Conf. Power Electron., Intell. Motion, Renew. Energy Energy Manage.*, May 2023, pp. 1–10. [Online]. Available: https://ieeexplore.ieee.org/document/10173420/

[15] M. A. Sakka, T. Geury, M. Dhaens, M. A. Sakka, M. E. Baghdadi, and O. Hegazy, "Reliability and cost assessment of fault-tolerant inverter topologies for multi-motor drive systems," in *Proc. 23rd Eur. Conf. Power Electron. Appl.*, Sep. 2021, pp. 1–10. [Online]. Available: https://ieeexplore.ieee.org/document/9570712/

[16] D. K. Murugesan and I. Manickam, "Reliability and cost analysis of different power inverter topologies in electric vehicles," in *Proc. IEEE Transp. Electrific. Conf. Exp (ITEC)*, Jun. 2015, pp. 1–4. [Online]. Available: https://ieeexplore.ieee.org/document/7165748/

[17] N. Christensen, S. Beczkowski, C. Uhrenfeldt, and S. Munk-Nielsen, "Cost, efficiency and power density Pareto investigation of three phase inverters," in *Proc. 20th Eur. Conf. Power Electron. Appl.*, Sep. 2018, pp. P.1–P.8. [Online]. Available: https://ieeexplore.ieee.org/document/8515314/

[18] M. Su, C. Chen, S. Sharma, and J. Kikuchi, "Performance and cost considerations for SiC-based HEV traction inverter systems," in *Proc. IEEE 3rd Workshop Wide Bandgap Power Devices Appl.*, Nov. 2015, pp. 347–350. [Online]. Available: https://ieeexplore.ieee.org/document/7369032/

[19] A. Mattsson, P. Nuutinen, P. Peltoniemi, T. Kaipia, J. Karppanen, V. Väisänen, J. Partanen, and P. Silventoinen, "Life-cycle cost analysis for the customer-end inverter used in low voltage DC distribution," in *Proc. IEEE 1st Int. Conf. DC Microgrids (ICDCM)*, Jun. 2015, pp. 148–153. [Online]. Available: https://ieeexplore.ieee.org/document/7152027/

[20] B. Baudais, H. B. Ahmed, G. Jodin, N. Degrenne, and S. Lefebvre, "Life cycle assessment of a 150 kW electronic power inverter," *Energies*, vol. 16, no. 5, p. 2192, Feb. 2023. [Online]. Available: https://www.mdpi.com/1996-1073/16/5/2192

[21] A. Accardo, E. Spessa, A. R. Martin, J. Essl, M. Duft, and J. Bachler, "Life cycle assessment of electric drivetrains for sustainable transport," in *Proc. Int. Conf. Elect. Mach. (ICEM)*, Sep. 2024, pp. 1–7. [Online]. Available: https://ieeexplore.ieee.org/document/10700391/

[22] P. Andrada, B. Blanqué, E. Martínez, J. I. Perat, J. A. Sánchez, and M. Torrent, "Environmental and life cycle cost analysis of one switched reluctance motor drive and two inverter-fed induction motor drives," *IET Electr. Power Appl.*, vol. 6, no. 7, pp. 390–398, Aug. 2012. [Online]. Available: https://digital-library.theiet.org/doi/10.1049/iet-epa.2011.0320

[23] L. Zanchi, M. Delogu, M. Ierides, and H. Vasiliadis, "Life cycle assessment and life cycle costing as supporting tools for EVs lightweight design," in *Sustainable Design and Manufacturing 2016*, R. Setchi, R. J. Howlett, Y. Liu, and P. Theobald, Eds., Cham, Switzerland: Springer, 2016, pp. 335–348.

[24] T. Liu, Y. Gu, G. Hu, Y. Wu, Q. Yuan, H. Hu, and T. Zuo, "Lifecycle eco-design potential of battery electric vehicles considering environmental and economic functions," *Resource Conservation Recycling*, vol. 224, Jan. 2026, Art. no. 108546. [Online]. Available: https://linkinghub.elsevier.com/retrieve/pii/S0921344925004239

[25] K. Petrauskienė, A. Galinis, D. Kliaugaitė, and J. Dvarionienė, "Comparative environmental life cycle and cost assessment of electric, hybrid, and conventional vehicles in Lithuania," *Sustainability*, vol. 13, no. 2, p. 957, Jan. 2021. [Online]. Available: https://www.mdpi.com/2071-1050/13/2/957

[26] J. Chen, X. Lai, Q. Chen, Y. Zheng, Y. Niu, L. Sun, B. Tang, and E. Cheng, "Unveiling the social and environmental benefits of electric vehicles: A case study of Shanghai," *J. Environ. Manage.*, vol. 393, Oct. 2025, Art. no. 127095. [Online]. Available: https://www.sciencedirect.com/science/article/pii/S0301479725030713

[27] J. Scholz, N. Klein, F. Kößler, and J. Fleischer, "Systematic digital twin-based development approach for holistic sustainable electric traction motors," *Sustainability*, vol. 17, no. 6, p. 2518, Mar. 2025.

[28] N. Di Vittorio, A. Accardo, E. Spessa, L. Viscido, and E. Tam, "LCA and LCC of a Li-ion battery pack for automotive application," *SAE Int. J. Adv. Current Practices Mobility*, vol. 6, no. 4, pp. 1995–2004, Aug. 2023. [Online]. Available: https://www.sae.org/content/2023-24-0170

[29] A. Accardo, G. Gentilucci, L. Pontone, and E. Spessa, "Investigating life cycle cost, environmental and social impacts of a lithium–ion battery pack," *IEEE Open J. Veh. Technol.*, vol. 6, pp. 1698–1709, 2025. [Online]. Available: https://ieeexplore.ieee.org/document/11031181/

[30] *14040 Environmental Management. Life Cycle Assessment. Principles and Framework*, oCLC Standard 401566895, ISO, Geneva, Switzerland, 2021. [Online]. Available: https://store.uni.com/uni-en-iso-14040-2021

[31] *14044 Environmental Management. Life Cycle Assessment. Requirements and Guidelines*, oCLC Standard 9521624510, ISO, Geneva, Switzerland, 2021. [Online]. Available: https://store.uni.com/uni-en-iso-14044-2021

[32] D. Hunkeler, K. Lichtenvort, and G. Rebitzer, *Environmental Life Cycle Costing*. Boca Raton, FL, USA: CRC Press, 2008. [Online]. Available: ww.setac.org

[33] R. Heijungs, E. Settanni, and J. Guinée, "Toward a computational structure for life cycle sustainability analysis: Unifying LCA and LCC," *Int. J. Life Cycle Assessment*, vol. 18, no. 9, pp. 1722–1733, Nov. 2013. [Online]. Available: http://link.springer.com/10.1007/s11367-012-0461-4

[34] T. E. Swarr, D. Hunkeler, W. Klöpffer, H.-L. Pesonen, A. Ciroth, A. C. Brent, and R. Pagan, "Environmental life-cycle costing: A code of practice," *Int. J. Life Cycle Assessment*, vol. 16, no. 5, pp. 389–391, Jun. 2011. [Online]. Available: http://link.springer.com/10.1007/s11367-011-0287-5

[35] F. Stella, E. Vico, D. Cittanti, C. Liu, J. Shen, and R. Bojoi, "Design and testing of an automotive compliant 800V 550 kVA SiC traction inverter with full-ceramic DC-link and EMI filter," in *Proc. IEEE Energy Convers. Congr. Exp. (ECCE)*, Oct. 2022, pp. 1–8. [Online]. Available: https://ieeexplore.ieee.org/document/9948096/

[36] P. K. Maroti, S. Padmanaban, M. S. Bhaskar, V. K. Ramachandaramurthy, and F. Blaabjerg, "The state-of-the-art of power electronics converters configurations in electric vehicle technologies," *Power Electron. Devices Compon.*, vol. 1, Mar. 2022, Art. no. 100001. [Online]. Available: https://www.sciencedirect.com/science/article/pii/S2772370421000018

[37] J. Reimers, L. Dorn-Gomba, C. Mak, and A. Emadi, "Automotive traction inverters: Current status and future trends," *IEEE Trans. Veh. Technol.*, vol. 68, no. 4, pp. 3337–3350, Apr. 2019. [Online]. Available: https://ieeexplore.ieee.org/document/8636258/

[38] G. Roos and E. M. D. Paolo. (Apr. 2022). *Under the Hood: The ID.3 and VW's Electrification Platform*. [Online]. Available: https://www.powerelectronicsnews.com/under-the-hood-the-id-3-and-vws-electrification-platform/

[39] Volkswagen. (2021). *The High-Voltage System in the ID.4*. Volkswagen Academy, Self Study Program SSP 811213. [Online]. Available: https://static.nhtsa.gov/odi/tsbs/2021/MC-10186407-0001.pdf

[40] Munro. (Jun. 2021). *Volkswagen ID.4 Electric Motor Teardown: A Modular Masterclass in Lean Design*. [Online]. Available: https://leandesign.com/volkswagen-id4-electric-motor-teardown/

[41] A. Nordelöf and M. Alatalo, "A scalable life cycle inventory of an automotive power electronic inverter unit—Technical and methodological description, version 1.01," Dept. of Energy and Environ. Divisions of Environ. Syst. Anal., Electr. Power Eng, Chalmers Univ. of Technol., Gothenburg, Sweden, Tech. Rep. 2016:5 (1.01), 2018, vol. 2016.

[42] A. Ciroth, J. Franze, and G. Berlin. (2009). *Life Cycle Costing in SimaPro*. [Online]. Available: https://pre-sustainability.com/files/2020/09/LCCinSimaPro_english.pdf
[43] Siemens. (2024). *Siemens Digital Industries Software*. [Online]. Available: https://www.siemens.com/en-us/products/teamcenter/solutions/product-cost-management/
[44] Fishersci. (2025). *Laboratory & Production Essentials*. [Online]. Available: https://www.fishersci.it/it/it/home.html
[45] Fibar. (May 2024). *Understanding the True Value: GFRP Cost Per KG and Its Impact on Construction Economy in India,*. [Online]. Available: https://wwwgetfibarcom/post/understanding-the-true-value-gfrp-cost-per-kg-and-its-impact-on-construction-economy-in-india/
[46] Octopart. (2025). *Schede Tecniche, Parti E Componenti Elettronici*. [Online]. Available: https://octopart.com/it/
[47] OilOnline. (2025). *Castrol Fuchs Houghton Klüber Mobil Shell Q8 Total*. [Online]. Available: https://www.oilonline.store/it/
[48] S. Sala, V. De Laurentiis, L. Zampori, E. Diaconu, S. Fazio, and F. Biganzioli, "Supporting information to the characterisation factors recommended EF life cycle impact assessment methods: Version 2, from ILCD to EF 3.0," Publications office of the European Union, Tech. Rep. EUR 29600 EN, 2018. [Online]. Available: https://data.europa.eu/doi/10.2760/002447
[49] Joint Research Centre. (2016). *Guide for Interpreting Life Cycle Assessment Result*. [Online]. Available: https://data.europa.eu/doi/10.2788/171315
[50] J. Haraldsson and M. T. Johansson, "Effects on primary energy use, greenhouse gas emissions and related costs from improving energy end-use efficiency in the electrolysis in primary aluminium production," *Energy Efficiency*, vol. 13, no. 7, pp. 1299–1314, Oct. 2020, doi: 10.1007/s12053-020-09893-1.
[51] G. Saevarsdottir, H. Kvande, and B. J. Welch, "Reducing the carbon footprint: Aluminium smelting with changing energy systems and the risk of carbon leakage," in *Proc. Light Metals*, A. Tomsett, Ed., Cham, Switzerland: Springer, 2020, pp. 726–734.
[52] G. Olivieri, A. Romani, and P. Neri, "Environmental and economic analysis of aluminium recycling through life cycle assessment," *Int. J. Sustain. Develop. World Ecol.*, vol. 13, no. 4, pp. 269–276, Aug. 2006. [Online]. Available: https://www.tandfonline.com/doi/abs/10.1080/13504500609469678
[53] F. Arfelli, D. Cespi, F. Codecà, and F. Passarini, "Life cycle assessment of a DC-LINK capacitor used for automotive applications," *J. Cleaner Prod.*, vol. 525, Sep. 2025, Art. no. 146486. [Online]. Available: https://www.sciencedirect.com/science/article/pii/S0959652625018360
[54] M. B. Mansilha, M. Brondani, F. A. Farret, L. C. da Rosa, and R. Hoffmann, "Life cycle assessment of electrical distribution transformers: Comparative study between aluminum and copper coils," *Environ. Eng. Sci.*, vol. 36, no. 1, pp. 114–135, Jan. 2019, doi: 10.1089/ees.2018.0256.
[55] Eurostat. (2022). *Simplified Energy Balances*. [Online]. Available: https://ec.europa.eu/eurostat/databrowser/product/page/NRGBALS
[56] B. Marmiroli, M. Messagie, G. Dotelli, and J. Van Mierlo, "Electricity generation in LCA of electric vehicles: A review," *Appl. Sci.*, vol. 8, no. 8, p. 1384, Aug. 2018. [Online]. Available: https://www.mdpi.com/2076-3417/8/8/1384
[57] Y. Yang, L. Dorn-Gomba, R. Rodriguez, C. Mak, and A. Emadi, "Automotive power module packaging: Current status and future trends," *IEEE Access*, vol. 8, pp. 160126–160144, 2020. [Online]. Available: https://ieeexplore.ieee.org/document/9178734/
[58] U. Scheuermann, "Packaging and reliability of power modules–principles, achievements and future challenges," in *Proc. PCIM Eur. Int. Exhib. Conf. Power Electron., Intell. Motion, Renew. Energy Energy Manage.*, May 2015, pp. 1–16. [Online]. Available: https://ieeexplore.ieee.org/document/7148819/
[59] J. Wang, H. Chen, and L. Wang, "Prediction of China's silicon wafer price: A GA-PSO-BP model," *Mathematics*, vol. 13, no. 15, p. 2453, Jul. 2025. [Online]. Available: https://www.mdpi.com/2227-7390/13/15/2453
[60] A. Varas, R. Varadarajan, J. Goodrich, and F. Yinug "Strengthening the global semiconductor supply chain in an uncertain era," Semiconductor Industry Association, Tech. Rep., Apr. 2021. [Online]. Available: http://www.semiconductors.org/strengthening-the-global-semiconductor-supply-chain-in-an-uncertain-era/
[61] K. B. Singh and S. C. Misra, "Manufacturing of semiconductor chips: From their origins to the current automotive chip crisis," *IEEE Eng. Manag. Rev.*, vol. 53, no. 5, pp. 260–273, Oct. 2025. [Online]. Available: https://ieeexplore.ieee.org/document/10745595/
[62] V. Ramani, D. Ghosh, and M. S. Sodhi, "Understanding systemic disruption from the COVID-19-induced semiconductor shortage for the auto industry," *Omega*, vol. 113, Dec. 2022, Art. no. 102720. [Online]. Available: https://www.sciencedirect.com/science/article/pii/S03050483220012 7X
[63] P. Nagapurkar and S. Das, "Economic and embodied energy analysis of integrated circuit manufacturing processes," *Sustain. Comput., Informat. Syst.*, vol. 35, Sep. 2022, Art. no. 100771. [Online]. Available: https://www.sciencedirect.com/science/article/pii/S2210537922001020
[64] H. Oh, B. Han, P. McCluskey, C. Han, and B. D. Youn, "Physics-of-failure, condition monitoring, and prognostics of insulated gate bipolar transistor modules: A review," *IEEE Trans. Power Electron.*, vol. 30, no. 5, pp. 2413–2426, May 2015. [Online]. Available: https://ieeexplore.ieee.org/document/6874580/
[65] E. Barbarini and F. Iannuzzo, "Prospects and outlooks in power electronics technology and market," in *Modern Power Electronic Devices: Physics, Applications, and Reliability*. Denmark: Alborg Universitet, Oct. 2020, pp. 451–467. [Online]. Available: https://digital-library.theiet.org/content/books/10.1049/pbpo152ech14
[66] Y. Wang, X. Dai, G. Liu, D. Li, and S. Jones, "An overview of advanced power semiconductor packaging for automotive system," in *Proc. 9th Int. Conf. Integr. Power Electron. Syst.*, Mar. 2016, pp. 1–6. [Online]. Available: https://ieeexplore.ieee.org/document/7736706/
[67] V. Veliadis, "SiC power device mass commercialization," in *Proc. IEEE 52nd Eur. Solid-State Device Res. Conf. (ESSDERC)*, Sep. 2022, pp. 31–36. [Online]. Available: https://ieeexplore.ieee.org/document/9947113/
[68] I. Aghabali, J. Bauman, P. J. Kollmeyer, Y. Wang, B. Bilgin, and A. Emadi, "800-V electric vehicle powertrains: Review and analysis of benefits, challenges, and future trends," *IEEE Trans. Transport Electrific.*, vol. 7, no. 3, pp. 927–948, Sep. 2021. [Online]. Available: https://ieeexplore.ieee.org/document/9294077
[69] D. Dutta, R. Rautela, L. K. S. Gujjala, D. Kundu, P. Sharma, M. Tembhare, and S. Kumar, "A review on recovery processes of metals from E-waste: A green perspective," *Sci. Total Environ.*, vol. 859, Feb. 2023, Art. no. 160391. [Online]. Available: https://www.sciencedirect.com/science/article/pii/S0048969722074939
[70] Businessanalytiq. (Sep. 2023). *Brass Price Index*. Accessed: Oct. 4, 2026. [Online]. Available: https://businessanalytiq.com/procurementanalytics/index/brass-price-index/
[71] London Metal Exchange. *LME Aluminium London Metal Exchange*. Accessed: Apr. 10, 2026. [Online]. Available: https://www.lme.com/Metals/Non-ferrous/LME-Aluminium
[72] Il Sole 24 ore. (2025). *Quotazione ORO in Tempo Reale: Prezzo Oro Al Grammo Oggi*. [Online]. Available: https://mercati.ilsole24ore.com/materie-prime/commodities/oro/GLDEUR
[73] Silmet. (2025). *Copper Quotations*. [Online]. Available: https://www.silmet.com/en/copper-quotations/
[74] S. Jasper, R. Subash, K. Muthuneelakandan, D. Vijayakumar, and S. J. Ida, "The mechanical properties of brass alloys: A review," *Eng. Proc.*, vol. 93, no. 1, p. 11, 2025. [Online]. Available: https://www.mdpi.com/2673-4591/93/1/11
[75] Scrap metal buyers. (2025). *Scrap Metal Prices*. [Online]. Available: https://scrapmetalbuyers.com/current-prices/
[76] P. Mercader-Moyano and P. Porras-Pereira, *Life Cycle Analysis Based on Nanoparticles Applied to the Construction Industry: A Comprehensive Curriculum*. Cham, Switzerland: Springer, 2025. [Online]. Available: https://link.springer.com/10.1007/978-3-031-79115-4
[77] Merck. (2025). *Acqua Sigma-Aldrich*. [Online]. Available: https://www.sigmaaldrich.com/IT/it/product/sigma/w3500
[78] S. Kokare, J. P. Oliveira, and R. Godina, "A LCA and LCC analysis of pure subtractive manufacturing, wire arc additive manufacturing, and selective laser melting approaches," *J. Manuf. Processes*, vol. 101, pp. 67–85, Sep. 2023. [Online]. Available: https://www.sciencedirect.com/science/article/pii/S1526612523005856
[79] H. Medarac, R. J. A. Moya, and J. Somers, "Production costs from iron and steel industry in the EU and third countries," Publications Office of the European Union, Luxembourg, Tech. Rep. EUR 30316 EN, 2020. [Online]. Available: https://publications.jrc.ec.europa.eu/repository/handle/JRC121276
[80] GlobalPetrolPrices. (2025). *Electricity Prices Around the World*. [Online]. Available: https://www.globalpetrolprices.com/electricityprices/

ANTONELLA ACCARDO received the M.S. degree in mechanical engineering from the Polytechnic of Turin, Italy, in 2019, and the Ph.D. degree from the Department of Energy, Polytechnic of Turin, in 2025. She is currently an Assistant Professor with the Department of Energy and a member of the Interdepartmental Center for Automotive Research and Sustainable Mobility (CARS). Her research interests focus on the sustainability of the transport sector, including the application of life cycle assessment and life cycle costing to light- and heavy-duty commercial vehicles and their main components.

FLAVIO CALVI received the M.S. degree in mechanical engineering from the Polytechnic of Turin, Italy, in 2024. He is currently pursuing the Ph.D. degree with the Department of Energy and a member of the Interdepartmental Center for Automotive Research and Sustainable Mobility (CARS). His research interests focus on the sustainability of the transport sector, including the application of life cycle assessment and life cycle costing to power electronics and powertrain components.

STEFANO E. ZUCCA was born in Rivoli, Italy, in 1997. He received the B.S. degree in mechanical engineering and the M.S. degree in mechanical engineering (land vehicle propulsion orientation) from the Polytechnic of Turin, in 2021 and 2025, respectively. He is currently a Junior Cost and Benchmarking Engineer with Dumarey Automotive Italia S.p.A.

GIANFRANCO MALAGRINÒ received the master's degree (Hons.) in propulsion systems from the Polytechnic of Turin. He is currently a Mechanical Engineer. He is also with Dumarey Automotive Italia S.p.A. He is experienced in cost engineering, competitive benchmarking, and sustainability assessment within the automotive industry. He has co-authored several technical articles focused on life cycle assessment and diesel combustion systems optimization.

MICHELE PENSATO was born in Foggia, Italy, in 1976. He received the master's degree in mechanical engineering from the Polytechnic of Turin, in 2002. He is currently a Cost and Benchmarking Manager.

SILVIO D. MOSSO was born in Torino in 1976. He received the degree in mechanical engineering from the Polytechnic of Turin, in 2003. He began his career in the automotive business industry as a Design Engineer with Fiat-GM Powertrain, Torino Mirafiori Plant. In 2005, he joined the newly established Diesel Engineering Center of GM Powertrain Europe, where he contributed on the design and the development of several new engine families. In 2017, he moved to the Cost Engineering Department as a Senior Cost Engineer for heads and blocks. In 2020, he joined Dumarey Automotive Italia S.p.A., as a Technical Leader for the Cost Engineering and Benchmarking Team.

LEONARDO TINACCI was born in Montevarchi, Arezzo, Italy, in 1974. He received the M.S. degree in electronic engineering from the University of Florence, Italy, in 2002. He is currently a Project Lead for Cost, Benchmarking, and Life Cycle Assessment (LCA) with Dumarey Automotive Italia S.p.A. He has more than 20 years of experience in the automotive industry, with particular expertise in powertrain systems, internal combustion engines, electrified propulsion technologies, product cost analysis, competitive benchmarking, and life cycle assessment.

EZIO SPESSA was born in Turin, Italy, in 1966. He received the degree (Hons.) in mechanical engineering and the Ph.D. degree in energetics from the Polytechnic of Turin, in 1991. He is currently a Full Professor with the Department of Energy "Galileo Ferraris," Polytechnic of Turin. His main expertise and research areas include LCA approaches and circular economy aspects for sustainable and innovative road mobility solutions.